

FIG 1 Replication and virus production by MA/JFH-1 chimeras in Huh7.5.1 cells. (A) Schematic structures of JFH-1, MA, and two MA/JFH-1 chimeras (MA/JFH-1.1 and MA/JFH-1.2). The junction of JFH-1 and MA in the 5' UTR is an AgeI site, and the junction of MA and JFH-1 in the NS2 region is a BsaBI site. A, AgeI; B, BsaBI; X, XbaI. (B to E) Chimeric HCV RNA replication in Huh7.5.1 cells. HCV core protein level in cells (B) and culture medium (C) and HCV RNA levels in medium (D) and infectivity of culture medium (E) from HCV RNA-transfected Huh7.5.1 cells are shown. Ten micrograms of HCV RNA was transfected into Huh7.5.1 cells, and cells and culture medium were harvested on days 1, 2, and 3. n.d., not determined. Assays were performed three times independently, and data are presented as means \pm standard deviation. Dashed line indicates detection limit. wt, wild type.

GGA AGT TCT GCT CGG CCC T-3' (sense) and 5'-AGA ACT TCC CCA CCT AGC CTC GCG GAA ACC G-3' (antisense); T1106A, 5'-CAG ATG TAC GCC AGC GCA GAG GGG GAC CTC-3' (sense) and 5'-CTG CGC TGG CGT ACA TCT GGG TGA CTG GTC-3' (antisense); and V1951A, 5'-GTG ACG CAG GCG TTA AGC TCA CTC ACA ATT ACC-3' (sense) and 5'-TGA GCT TAA CGC CTG CGT CAC GCG CAG CGA G-3' (antisense). To construct the MA chimeric virus harboring minimal regions of JFH-1 (MA/N3H+N5BX-JFH1), ClaI (nt 3930), EcoT22I (nt 5294), and BsrGI (nt 7782) recognition sites were introduced into pMA by site-directed mutagenesis. The 5' UTR (EcoRI-AgeI), the region of the NS3 helicase (N3H; ClaI-EcoT22I), and the region of NS5B to 3' X (N5BX;

BsrGI-XbaI) were then replaced with the corresponding regions from JFH-1.

RNA synthesis, transfection, and determination of infectivity. RNA synthesis and transfection were performed as described previously (12, 22). Determination of infectivity was also performed as described previously, with infectivity expressed as the number of focus-forming units per milliliter (FFU/ml) (12, 22). When necessary, culture medium was concentrated 20-fold in Amicon Ultra-15 spin columns (100-kDa molecular-weight-cutoff; Millipore, Bedford, MA) in order to determine infectivity.

Quantification of HCV core protein and HCV RNA. In order to estimate the concentration of HCV core protein in culture medium, we performed a chemiluminescence enzyme immunoassay (Lumipulse II HCV core assay; Fujirebio, Tokyo, Japan) in accordance with the manufacturer's instructions. HCV RNA from harvested cells or culture medium was isolated using an RNeasy Mini RNA kit (Qiagen, Tokyo, Japan) or QiaAmp Viral RNA Minikit (Qiagen), respectively. Copy number of HCV RNA was determined by real-time quantitative reverse transcription-PCR (qRT-PCR), as described previously (28).

HCV sequencing. Total RNA in culture supernatant was extracted with Isogen-LS (Nippon Gene Co., Ltd., Tokyo, Japan). cDNA was synthesized using Superscript III Reverse Transcriptase (Invitrogen, Carlsbad, CA). cDNA was subsequently amplified with LA Taq DNA polymerase (TaKaRa, Shiga, Japan). Four separate PCR primer sets were used to amplify the fragments of nt 130 to 2909, 2558 to 5142, 4784 to 7279, and 7081 to 9634 covering the entire open reading frame and part of the 5' UTR and 3' UTR of the MA strain. Sequences of amplified fragments were determined directly.

Immunostaining. Infected cells were cultured on Multitest Slides (MP Biomedicals, Aurora, OH) and were fixed in acetone-methanol (1:1, vol/vol) for 15 min at -20°C . After a blocking step, infected cells were visualized with anti-core protein antibody (clone 2H9) (29) and Alexa Fluor 488 goat anti-mouse IgG (Invitrogen), and nuclei were visualized with 4',6'-diamidino-2-phenylindole (DAPI).

Assessment of interferon sensitivity. Two micrograms of *in vitro* transcribed RNA was transfected into 3×10^6 Huh7.5.1 cells. Four hours after transfection, cells were placed in fresh medium or medium containing 0.1, 1, 10, 100, and 1,000 IU/ml of interferon α -2b (Intron A; Schering-Plough Corporation, Osaka, Japan). Culture medium was then harvested on day 3, and HCV core levels in the cells and in the medium were measured.

Statistical analysis. Significant differences were evaluated by Student's *t* test. A *P* value of <0.05 was considered significant.

RESULTS

Transient replication and production of 2b/2a chimeric virus.

We first tested whether the MA strain (genotype 2b) (19) was able to replicate and produce infectious virus in cultured cells. When the *in vitro* transcribed RNA of MA was transfected into Huh7.5.1 cells, a highly HCV-permissive cell line, replication and virus production were not observed (Fig. 1A to C). We then tested whether 2b/2a chimeric RNA harboring the structural region (5' UTR to E2) of the MA strain and the nonstructural region (p7 to 3' UTR) of JFH-1 (Fig. 1A, MA/JFH-1.1) was able to replicate in the cells. After MA/JFH-1.1 RNA transfection, time-dependent accumulation of core protein in the cells (Fig. 1B) and culture medium (Fig. 1C) was observed, indicating that MA/JFH-1.1 RNA was able to replicate in the cells autonomously. HCV RNA levels in the medium were determined by qRT-PCR, and time-dependent increases in HCV RNA level were also observed (Fig. 1D). Infectious virus production was observed on day 3, but infectivity was 17.6-fold lower than that of JFH-1 (Fig. 1E).

In order to improve the level of infectious virus production, we tested another chimeric construct, MA/JFH-1.2, which contained an additional MA-to-JFH-1 replacement of the 5' UTR (Fig. 1A),

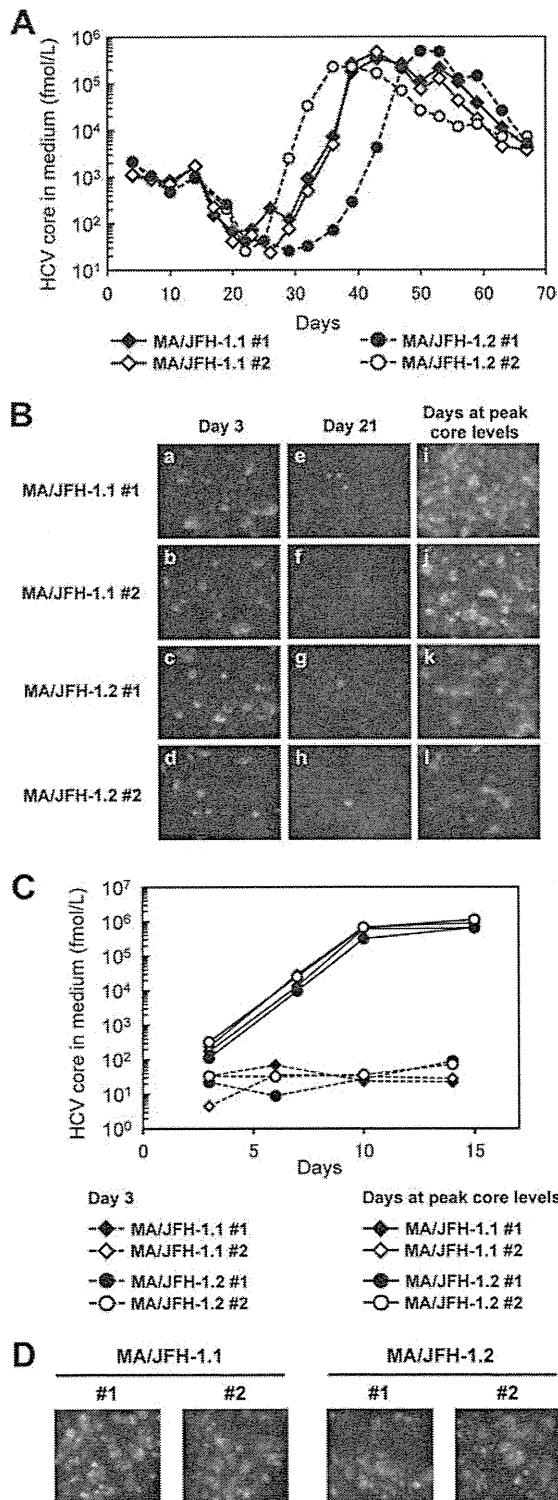


FIG 2 Long-term culture of MA/JFH-1.1 and MA/JFH-1.2 RNA-transfected cells. Ten micrograms of HCV RNA was transfected into Huh7.5.1 cells, and cells were passaged every 2 to 5 days, depending on cell status. Culture medium was collected after every passage, and HCV core protein levels were measured. Transfection was performed twice for each chimeric RNA (1 and 2 for each construct). (A) HCV core protein levels in culture medium from MA/JFH-1.1 and MA/JFH-1.2 RNA-transfected cells. (B) Immunostained cells at 3 days after transfection (a to d), at 21 days after transfection (e to h), and at the time

TABLE 1 HCV core protein levels and infectivity in culture medium immediately after RNA transfection (day 3) and after long-term culture (days 35 to 49)

Sample period and virus	Sample no.	Day no. ^a	HCV core (fmol/liter)	Infectivity (FFU/ml)
After transfection				
MA/JFH-1.1	1	3	1.06×10^3	5.00×10^1
	2	3	1.14×10^3	5.70×10^1
MA/JFH-1.2	1	3	2.14×10^3	7.30×10^1
	2	3	2.15×10^3	9.30×10^1
After long-term culture				
MA/JFH-1.1	1	42	3.38×10^5	1.62×10^5
	2	42	4.70×10^5	3.23×10^5
MA/JFH-1.2	1	35	2.27×10^5	1.61×10^5
	2	49	4.93×10^5	3.27×10^5

^a For the long-term culture, the days are those of peak core protein levels.

as a 5' UTR replacement from J6CF (genotype 2a) to JFH-1 enhanced virus production of chimeric J6CF virus harboring the region of NS2 to 3' X of JFH-1 (J6/JFH-1) (A. Murayama et al., unpublished data). The core protein accumulation levels with MA/JFH-1.2 RNA-transfected cells were higher than those with MA/JFH-1.1 ($P < 0.05$) (Fig. 1B). Similarly, core protein and HCV RNA levels in the medium of MA/JFH-1.2 RNA-transfected cells were higher than those of MA/JFH-1.1 ($P < 0.05$) (Fig. 1C and D). Infectivity on day 3 was also higher than with MA/JFH-1.1 ($P < 0.05$) (Fig. 1E), indicating that the 5' UTR of JFH-1 enhanced virus production. However, infectivity of medium from MA/JFH-1.2 RNA-transfected cells on day 3 remained 6.4-fold lower than that of JFH-1 although HCV RNA levels in the medium were similar to those of JFH-1 (Fig. 1D and E).

These results indicate that 2b/2a chimeric RNA is able to replicate autonomously in Huh7.5.1 cells and produce infectious virus although infectivity remains lower than that of JFH-1.

Assembly-enhancing mutation in core region introduced during long-term culture. Because MA/JFH-1.1 and MA/JFH-1.2 replicated efficiently but produced small amounts of infectious virus, we performed long-term culture of these RNA-transfected cells in order to examine whether these chimeric RNAs would continue replicating and producing infectious virus over the long term. We prepared two RNA-transfected cell lines for each construct (MA/JFH-1.1 and MA/JFH-1.2) as both of these replicated and produced infectious virus at different levels.

Immediately after transfection, core protein levels and infectivity in culture medium were low (1.06×10^3 to 2.15×10^3 fmol/liter and 5.00×10^1 to 9.30×10^1 FFU/ml, respectively) (Fig. 2A and Table 1) although a considerable number of core protein-positive cells were observed by immunostaining (Fig. 2B, frames a to d). Subsequently, core protein levels in the culture medium decreased gradually (Fig. 2A), and core protein-positive cells were rare (Fig. 2B, frames e to h). However, at 30 to 40 days

of peak core levels (days 42 to 49). Infected cells were visualized with anti-core protein antibody (green), and nuclei were visualized with DAPI (blue). (C) Infection of naïve cells by culture medium at an MOI of 0.001. (D) Immunostained cells at 15 days after infection with medium at peak core protein levels (Fig. 2A) at an MOI of 0.001. Infected cells were visualized with anti-core antibody (green), and nuclei were visualized with DAPI (blue).

after transfection, core protein levels in the supernatants of all chimeric RNA-transfected cells increased and reached 2.27×10^5 to 4.93×10^5 fmol/liter (Fig. 2A and Table 1). Infectivity in the culture medium also increased (1.61×10^5 to 3.27×10^5 FFU/ml) (Table 1), and at this point, most of the cells were core protein positive (Fig. 2B, frame i to l).

As the infectivity of culture supernatant of MA/JFH-1 RNA-transfected cells appeared to increase after long-term culture, we compared viral spread by infection with these supernatants on day 3 (immediately after transfection) and for each peak in core protein levels (after long-term culture). When naïve Huh7.5.1 cells were infected with supernatant on days corresponding to a peak in core protein levels at a multiplicity of infection (MOI) of 0.001, core protein levels in the medium increased rapidly and reached 0.64×10^6 to 1.13×10^6 fmol/liter by day 15 after infection (Fig. 2C). Immunostained images showed that most cells were HCV core protein positive on day 15 (Fig. 2D). When naïve Huh7.5.1 cells were infected with supernatant from day 3 at an MOI of 0.001, core protein levels in the medium did not increase under these conditions (Fig. 2C). These results indicate that both MA/JFH-1 chimeric viruses (MA/JFH-1.1 and MA/JFH-1.2) acquired the ability to spread rapidly after long-term culture.

As the characteristics of the MA/JFH-1 virus changed in long-term culture, we analyzed the possible mutations in the viral genome from the supernatant at each peak in core protein levels (Table 1, days at peak core levels). Nine- to 12-nucleotide mutations were found in the viral genome from each supernatant, and the detected mutations were distributed along the entire genome. Among these mutations, a common nonsynonymous mutation was found in the core region (Arg to Gly at amino acid [aa]167, R167G).

In order to test the effects of R167G on virus production, an R167G substitution was introduced into MA/JFH-1.2 as MA/JFH-1.2/R167G replicated and produced infectious virus more efficiently than MA/JFH-1.1. HCV core protein levels in cells and medium of MA/JFH-1.2 with R167G (MA/JFH-1.2/R167G) were higher than with MA/JFH-1.2 ($P < 0.05$) (Fig. 3A and B). HCV RNA levels in the medium of MA/JFH-1.2/R167G RNA-transfected cells were also higher than with MA/JFH-1.2 ($P < 0.05$) (Fig. 3C). Infectious virus production was also increased by the R167G mutation ($P < 0.05$) (Fig. 3D) and was 8.7-fold higher than that of JFH-1 RNA-transfected cells on day 3 ($P < 0.05$) (Fig. 3D).

We then tested whether R167G was responsible for the rapid spread observed in culture supernatant after long-term culture by monitoring virus spread after infection of naïve Huh7.5.1 with culture medium taken 3 days after RNA transfection of MA/JFH-1.2 and MA/JFH-1.2/R167G at an MOI of 0.005. Core protein levels in medium from MA/JFH-1.2/R167G-infected cells increased with the same kinetics as levels of JFH-1 (Fig. 3E), and the population of core protein-positive cells was almost the same as with JFH-1-infected cells (Fig. 3F), indicating that MA/JFH-1.2/R167G virus spread as rapidly as JFH-1 virus. In contrast, we observed no infectious foci in the MA/JFH-1.2 virus-inoculated cells (Fig. 3F). These data suggest that the R167G mutation in the core region was a cell culture-adaptive mutation and that it enhanced infectious MA/JFH-1.2 virus production.

In order to determine whether R167G enhances RNA replication or other steps in the viral life cycle, we performed a single-cycle virus production assay (11) using Huh7-25 cells, a HuH-7-derived cell line lacking CD81 expression on the cell surface (1).

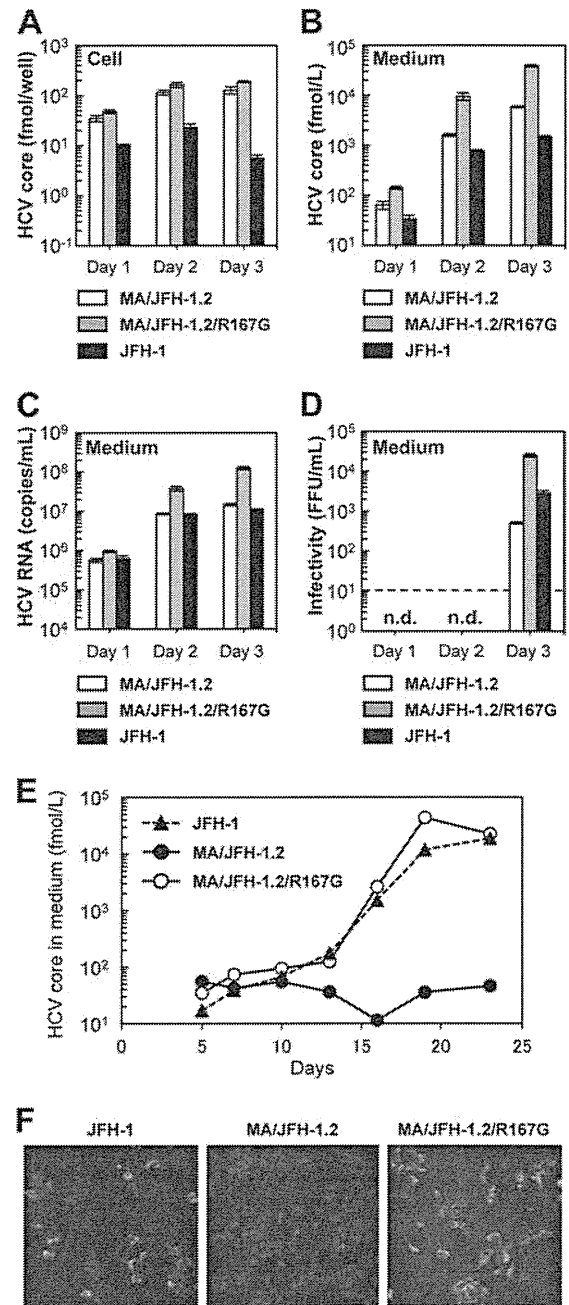


FIG 3 Effects of R167G on replication and virus production of MA/JFH-1.2 in Huh7.5.1 cells. Ten micrograms of HCV RNA was transfected into Huh7.5.1 cells, and cells and medium were harvested on days 1, 2, and 3. HCV core protein levels in the cells (A) and culture medium (B) and HCV RNA levels in the medium (C) and the infectivity of culture medium (D) from HCV RNA-transfected Huh7.5.1 cells are shown. n.d., not determined. Dashed line indicates the detection limit. Assays were performed three times independently, and data are presented as means \pm standard deviation. (E) HCV core protein levels in culture medium from cells infected with medium at 3 days posttransfection at an MOI of 0.005. (F) Immunostained cells at 19 days postinfection. Infected cells were visualized with anti-core antibody (green), and nuclei were visualized with DAPI (blue).

This cell line can support replication and infectious virus production upon transfection of HCV genomic RNA but cannot be reinfectious by progeny virus, thereby allowing observation of a single cycle of infectious virus production without the confounding ef-

fects of reinfection. R167G did not affect HCV core protein levels in the chimeric RNA-transfected Huh7-25 cells (Fig. 4A), demonstrating that R167G did not enhance RNA replication. Nevertheless, R167G increased HCV core protein levels in the medium ($P < 0.05$ on days 2 and 3) and infectivity (Fig. 4B and C). These results suggest that R167G did not affect RNA replication but affected other steps such as virus assembly and/or virus secretion.

Virus particle assembly efficiency was then assessed by determining intracellular-specific infectivity from infectivity and RNA titer in the cells, as reported previously (11). As shown in Fig. 4G, R167G enhanced intracellular-specific infectivity of MA/JFH-1.2 virus 10.2-fold. Virus secretion efficiency was also calculated from the amount of intracellular and extracellular infectious virus, but R167G had no effect (Fig. 4G).

To confirm the effects of Arg167 in other HCV strains, we tested its effects on JFH-1. As aa 167 of JFH-1 is Gly, we replaced it with Arg (G167R). HCV core protein levels in the cells were not affected by G167R (Fig. 4D), and no effects on RNA replication were confirmed. HCV core protein levels in the medium and infectivity decreased after G167R mutation (Fig. 4E and F). As the G167R mutation decreased intracellular infectious virus production of JFH-1 to undetectable levels, we were unable to determine the intracellular-specific infectivity and virus secretion efficiency of JFH-1 G167R (Fig. 4G). These results indicate that Gly is favored over Arg at core position 167 for infectious virus assembly in multiple HCV strains.

MA harboring the R167G mutation, 5' UTR, and N3H (NS3 helicase) and N5BX (NS5B to 3' X) regions of JFH-1 replicated and produced infectious chimeric virus. In order to establish a genotype 2b cell culture system with the MA strain with minimal regions of JFH-1, we attempted to reduce JFH-1 content in MA/JFH-1.2. We previously reported that replacement of the N3H and N5BX regions of JFH-1 allowed efficient replication of the J6CF strain, which normally cannot replicate in cells (21). Thus, we tested whether the N3H and N5BX regions of JFH-1 could also support MA RNA replication.

We prepared two chimeric MA constructs harboring the 5' UTR and N3H and N5BX regions of JFH-1, MA/N3H+N5BX-JFH1 (Fig. 5A) and MA/N3H+N5BX-JFH1/R167G. After *in vitro* transcribed RNA was transfected into Huh7.5.1 cells, intracellular core protein levels of MA/N3H+N5BX-JFH1 and MA/N3H+N5BX-JFH1/R167G RNA-transfected cells increased in a time-dependent manner and reached almost the same levels as with MA/JFH-1.2 RNA-transfected cells on day 5 (Fig. 5B). Extracellular core protein and HCV RNA levels of MA/N3H+N5BX-JFH1 and MA/N3H+N5BX-JFH1/R167G RNA-transfected cells also increased in a time-dependent manner (Fig. 5C and D). However, they were more than 10 times lower than with MA/JFH-1.2 RNA-transfected cells although intracellular core levels were comparable on day 5 (Fig. 5B to D).

We then tested whether the medium from MA/N3H+N5BX-JFH1 and MA/N3H+N5BX-JFH1/R167G RNA-transfected cells was infectious. Infectivity of the medium from MA/N3H+N5BX-JFH1 RNA-transfected cells was below the detection limit, and that of MA/N3H+N5BX-JFH1/R167G RNA-transfected cells on day 5 was very low ($3.3 \times 10^1 \pm 2.1 \times 10^1$ FFU/ml) (Fig. 5E). To confirm infectivity, the culture media were concentrated, and their infectivity was determined. Infected foci were observed after infection with concentrated medium in MA/N3H+N5BX-JFH1/R167G RNA-transfected cells (Fig. 5F), and infectivity was found

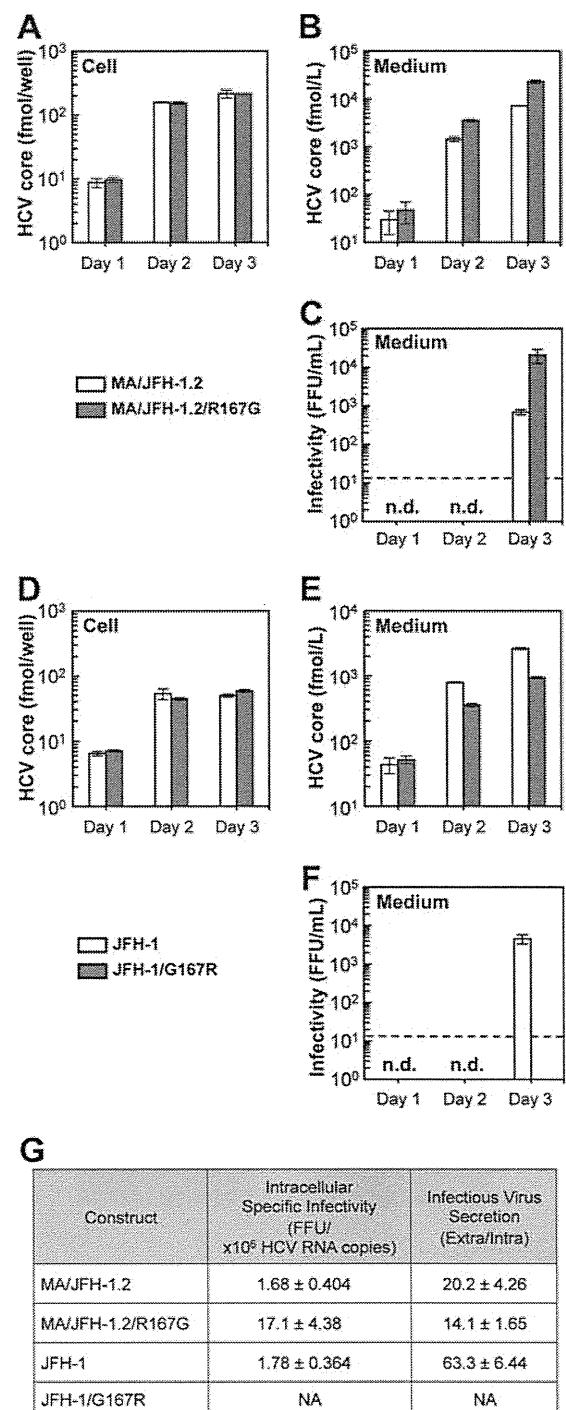


FIG 4 Effects of R167G on replication and virus production of MA/JFH-1.2 and JFH-1 in Huh7-25 cells. Ten micrograms of HCV RNA was transfected into Huh7-25 cells, and cells and medium were harvested on days 1, 2, and 3. HCV core protein levels in cells (A and D) and in medium (B and E) were measured, and infectivity of medium (C and F) was determined. n.d., not determined. Dashed line indicates the detection limit. (G) Intracellular specific infectivity and virus secretion efficiency of chimeric HCV RNA-transfected cells. Intracellular and extracellular infectivity of day 3 samples was determined, and specific infectivity and virus secretion rate were calculated. Assays were performed three times independently, and data are presented as means \pm standard deviation. NA, not available.

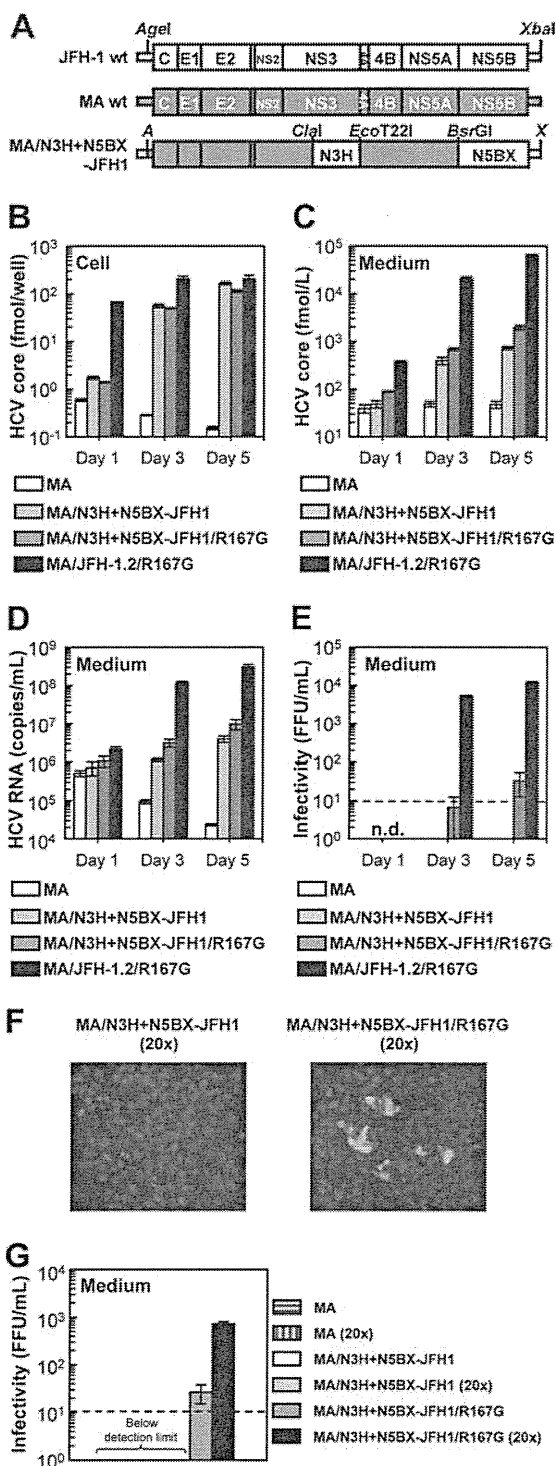


FIG 5 Replication and virus production of MA/N3H+N5BX-JFH1/R167G in Huh7.5.1 cells. (A) Schematic structures of JFH-1, MA, and MA/N3H+N5BX-JFH1. The junction of JFH-1 and MA in the 5' UTR is an AgeI site; the junctions of MA and JFH-1 in the NS3 regions are ClaI and EcoT22I sites, and the junction in the NS5B region is a BsrGI site. A, AgeI; X, XbaI. (B to G) Chimeric HCV RNA replication in Huh7.5.1 cells. Ten micrograms of HCV RNA was transfected into Huh7.5.1 cells, and cells and medium were harvested on days 1, 3, and 5. HCV core protein levels in cells (B) and in medium (C) and HCV RNA levels in medium (D) were measured, and infectivity of medium (E) was determined. Assays were performed three times independently, and data are presented as means \pm standard deviation. n.d., not determined. Dashed line indicates the detection limit. (F) Immunostained cells. Huh7.5.1

to be $7.27 \times 10^2 \pm 7.57 \times 10^1$ FFU/ml (Fig. 5G). No infected foci were observed after infection of MA/N3H+N5BX-JFH1 RNA-transfected cells, even when medium was concentrated (Fig. 5F), although intracellular and extracellular core protein levels were comparable to those with MA/N3H+N5BX-JFH1/R167G RNA-transfected cells (Fig. 5B and C). These results indicate that replacement of the 5' UTR and N3H and N5BX regions in JFH-1 were necessary to rescue autonomous replication in the replication-incompetent MA strain and for secretion of infectious chimeric virus. However, the secretion and infection efficiencies of the virus were low.

Cell culture-adaptive mutations enhanced infectious virus production of MA/N3H+N5BX-JFH1/R167G. Because MA/N3H+N5BX-JFH1/R167G replicated efficiently but produced very small amounts of infectious virus, we performed a long-term culture of the RNA-transfected cells in order to induce cell culture-adaptive mutations that could enhance infectious virus production. We prepared RNA-transfected cells using two constructs, MA/N3H+N5BX-JFH1 and MA/N3H+N5BX-JFH1/R167G; both of these replicated efficiently, and MA/N3H+N5BX-JFH1/R167G produced infectious virus at low levels while MA/N3H+N5BX-JFH1 did not. Immediately after transfection, the HCV core protein levels in the medium of each RNA-transfected cell culture peaked at 3.0×10^3 fmol/liter and declined thereafter. However, the core protein level in the medium with MA/N3H+N5BX-JFH1/R167G RNA-transfected cells continued to increase and reached a peak of 2.7×10^5 fmol/liter 54 days after transfection, at which point most cells were core protein positive (Fig. 6B). The core protein level in the medium with MA/N3H+N5BX-JFH1 RNA-transfected cells did not increase and core-positive cells were scarce on day 54 (Fig. 6B). We analyzed the viral genome in the culture supernatants from day 54 for possible mutations and identified four nonsynonymous mutations in the MA/N3H+N5BX-JFH1/R167G genome: L814S (NS2), R1012G, (NS2), T1106A (NS3), and V1951A (NS4B). In order to test whether these amino acid substitutions enhance infectious virus production, L814S, R1012G, T1106A, and V1951A were introduced into MA/N3H+N5BX-JFH1/R167G, and the product was designated MA/N3H+N5BX-JFH1/5am (where am indicates adaptive mutation). On day 1, although HCV core protein levels in the MA/N3H+N5BX-JFH1/5am RNA-transfected cells were higher than those of MA/N3H+N5BX-JFH1/R167G RNA-transfected cells, they were still lower than those of MA/JFH-1.2/R167G RNA-transfected cells; however, on days 3 and 5, they reached a level comparable to that of MA/JFH-1.2/R167G RNA-transfected cells (Fig. 6C). HCV core protein and HCV RNA levels in the medium of MA/N3H+N5BX-JFH1/5am RNA-transfected cells were higher than those of MA/JFH-1.2/R167G RNA-transfected cells ($P < 0.05$, Fig. 6D and 6E, respectively). MA/N3H+N5BX-JFH1/5am, containing the four additional adaptive mutations, produced infectious virus at the same level as MA/JFH-1.2/R167G on day 5 (Fig. 6F). These results indicate that the

cells were infected with concentrated medium from RNA-transfected cells on day 5. Infected cells were visualized with anti-core antibody (green), and nuclei were visualized with DAPI (blue). (G) Infectivity of concentrated culture medium from HCV RNA-transfected cells. Culture medium was concentrated by 20 times. Infectivities of original and concentrated culture media were determined. Dashed line indicates detection limit.

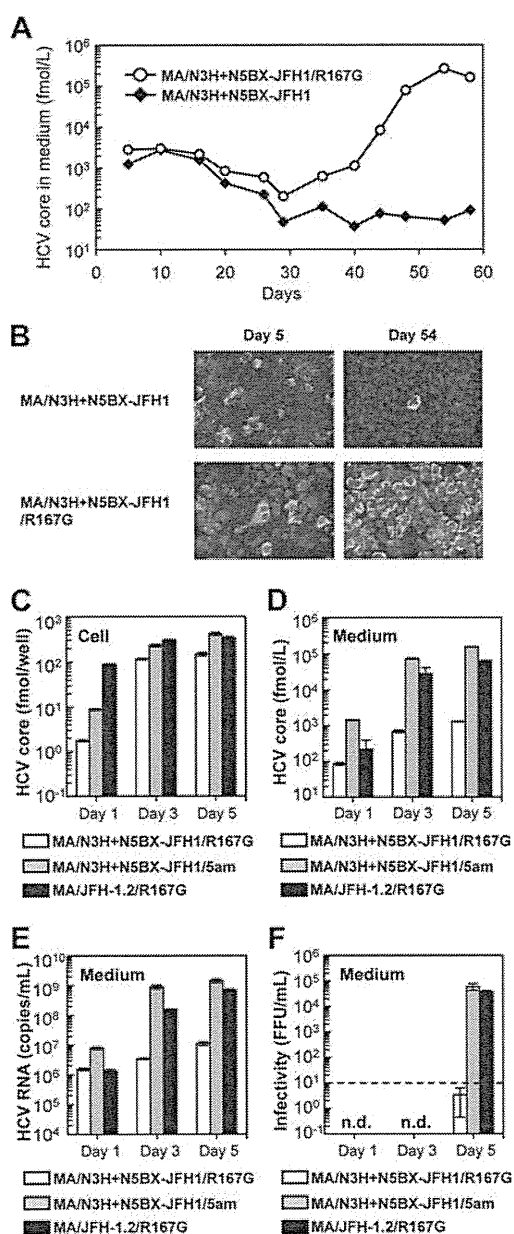


FIG 6 Cell culture-adaptive mutations enhanced infectious virus production of MA/N3H+N5BX-JFH1/R167G. (A) Long-term culture of MA/N3H+N5BX-JFH1 and MA/N3H+N5BX-JFH1/R167G RNA-transfected cells. Ten micrograms of HCV RNA was transfected into Huh7.5.1 cells, and cells were passaged every 2 to 5 days, depending on cell status. Culture medium was collected after every passage, and HCV core protein levels were measured. HCV core protein levels in culture medium from MA/N3H+N5BX-JFH1 and MA/N3H+N5BX-JFH1/R167G RNA-transfected cells are presented. (B) Immunostained cells on days 5 and 54 after transfection. Infected cells were visualized with anti-core antibody (green), and nuclei were visualized with DAPI (blue). (C to F) Effect of four additional cell culture-adaptive mutations on virus production. Ten micrograms of HCV RNA was transfected into Huh7.5.1 cells, and cells and medium were harvested on days 1, 3, and 5. HCV core levels in cells (C) and in medium (D) and HCV RNA levels in medium (E) were measured, and infectivity of medium (F) was determined. Assays were performed three times independently, and data are presented as means \pm standard deviation. n.d., not determined. Dashed line indicates the detection limit.

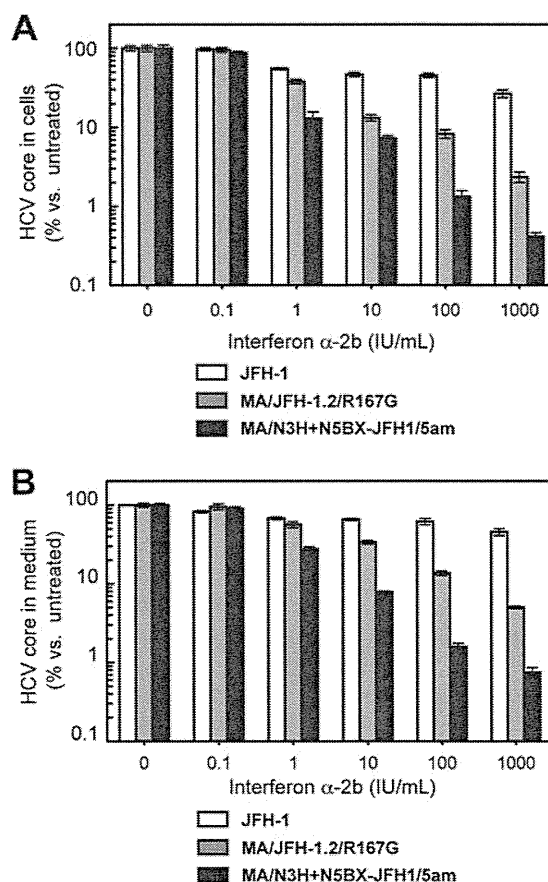


FIG 7 Comparisons of interferon sensitivity between JFH-1, MA/JFH-1.2/R167G and MA/N3H+N5BX-JFH1/5am. Two micrograms of HCV RNA was transfected into Huh7.5.1 cells, and interferon was added at the indicated concentrations at 4 h after transfection. HCV core protein levels in cells (A) and in medium (B) on day 3 were measured, and data are expressed as percent versus untreated cells (0 IU/ml). Assays were performed three times independently, and data are presented as means \pm standard deviation.

four additional adaptive mutations enhance infectious virus production and that MA/N3H+N5BX-JFH1/5am RNA-transfected cells replicate and produce infectious virus as efficiently as MA/JFH-1.2/R167G RNA-transfected cells.

Comparison of interferon sensitivity between JFH-1, MA/JFH-1.2/R167G, and MA/N3H+N5BX-JFH1/R167G. Using the newly established genotype 2b infectious chimeric virus, we compared interferon sensitivity between the JFH-1, MA/JFH-1.2/R167G, and MA/N3H+N5BX-JFH1/5am viruses. JFH-1 or MA chimeric viral RNA-transfected Huh7.5.1 cells were treated with 0.1, 1, 10, 100, or 1,000 IU/ml interferon α -2b, and HCV core protein levels in the cells and in culture media were compared. Interferon decreased HCV core protein levels in the JFH-1 RNA-transfected cells and in the medium in a dose-dependent manner, and production was inhibited to 26.8% \pm 3.0% and 45.6% \pm 4.7%, respectively, of control levels (Fig. 7A and B, respectively). In contrast, HCV core protein levels in cells and medium of MA/JFH-1.2/R167G and MA/N3H+N5BX-JFH1/5am RNA-transfected cells decreased more pronouncedly in a dose-dependent manner (Fig. 7A and B, respectively). HCV core protein levels in cells and medium from MA/N3H+N5BX-JFH1/5am RNA-transfected cells were lower than those from MA/JFH-1.2/

R167G RNA-transfected cells (Fig. 7A and B, respectively) ($P < 0.05$ at 1, 10, 100, and 1,000 IU/ml), indicating that the MA/N3H+N5BX-JFH1/5am virus was more sensitive to interferon than the MA/JFH1.2/R167G virus, which contained more regions from JFH-1.

DISCUSSION

In this study, we developed a novel infectious HCV production system using a genotype 2b chimeric virus. To improve infectious virus production, we introduced two modifications into the chimeric genome.

First, we replaced the 5' UTR from MA with that of JFH-1. Similarly to J6/JFH-1, replacement of the 5' UTR increased core protein accumulation in both the cells and medium when these RNAs were transfected into Huh7.5.1 cells (Fig. 1). The same trend was observed when these RNAs were transfected into Huh7-25 cells (data not shown), indicating that the 5' UTR of JFH-1 enhanced RNA replication. There are two genetic variations in J6CF and seven in MA in the region we replaced (nt 1 to 154 for J6CF and nt 1 to 155 for MA), and some of these mutations may affect RNA replication by changing the RNA secondary structure, RNA-RNA interactions, or binding of host or viral proteins.

Second, we introduced a cell culture-adaptive mutation (R167G) in the core region. This mutation was induced by long-term culture of MA/JFH-1 RNA-transfected cells (Fig. 2). MA/JFH-1 chimeric RNA (MA/JFH-1.1 and MA/JFH-1.2) replicated when synthesized RNA was transfected into the cells. However, infectious virus production was low, and virus infection did not spread over the short term. In early stages of long-term culture, the number of core protein-positive cells gradually decreased, and core protein-positive cells were scarcely detectable. Subsequently, the population of core protein-positive cells increased, reaching almost 100%. At this time point, we identified a common mutation in the core region (R167G) of the viral genome as a cell culture-adaptive mutation and found that it enhanced infectious virus production (Fig. 3). Several nonsynonymous mutations other than R167G were identified in the viral genome from each supernatant, and these mutations may enhance infectious virus production. However, there was a discrepancy between RNA levels and the infectivity of the culture media of MA/JFH-1.2 and MA/JFH-1.2/R167G RNA-transfected cells (Fig. 3C and D). The MA/JFH-1.2/R167G mutant had a 2-log increase in viral infectivity compared to that of MA/JFH-1.2 but only a 1-log increase in secreted RNA. The replication efficiency of MA/JFH-1.2 RNA-transfected cells was comparable to that of MA/JFH-1.2/R167G RNA-transfected cells, but the efficiency of infectious virus assembly within the cells was low, indicating that mainly noninfectious virus may be produced.

Infection of MA/JFH-1.2/R167G virus spreads rapidly, similarly to that of the JFH-1 virus, when it is inoculated into naïve Huh7.5.1 cells. On a single-cycle virus production assay, we found that the R167G mutation did not affect RNA replication or virus secretion but enhanced infectious virus assembly within the cells (Fig. 4). Efficient infectious virus assembly within the cells was mainly responsible for the rapid spread and high virus production of MA/JFH-1.2/R167G.

The amino acid at 167 (aa 167) is located in domain 2 of the core region, which is important for localization of the core

protein (3, 8). Lipid droplet localization of the core protein and/or NS5A is important for infectious virus production (4, 18, 26). The interaction between the core protein and NS5A is also important for infectious virus production (16). Thus, aa 167 affects infectious virus production possibly by altering sub-cellular localization of the core protein or interaction between the core protein and NS5A. We examined the amino acid sequence of the core protein in 2,078 strains in the Hepatitis Virus Database (<http://s2as02.genes.nig.ac.jp/>) and found that aa 167 is Gly in all other strains. These data strongly suggest that Gly at aa 167 is important for the HCV life cycle. As the MA strain was cloned from the serum of a patient with chronic hepatitis C, the low virus production by this Gly at aa 167 may be important for persistent infection.

We then attempted to reduce the contents of JFH-1 from MA/JFH-1.2/R167G. We previously reported that the N3H and N5BX regions of JFH-1 were sufficient for replication of the J6CF strain (21). We also reported that this effect was observed only in genotype 2a strains (J6CF, JCH-1, and JCH-4). In this study, we tested whether the N3H and N5BX regions of JFH-1 could also support replication of a genotype 2b strain, MA. We constructed an MA chimeric virus harboring the N3H and N5BX regions of JFH-1 and combined this with the 5' UTR of JFH-1 and the R167G mutation (MA/N3H+N5BX-JFH1/R167G). This chimeric RNA was able to replicate in the cells and produce infectious chimeric virus in culture medium although infectious virus production levels were low (Fig. 5).

We showed in this paper that the N3H and N5BX regions of JFH-1 were able to support RNA replication by both genotype 2a clones and genotype 2b clones, but the nucleotide sequence similarity between JFH-1 and MA was lower than that between JFH-1 and J6CF (77% versus 89%, respectively). Compared to MA/JFH-1.2/R167G, MA/N3H+N5BX-JFH1/R167G RNA showed the same levels of RNA replication and low levels of infectious virus production. To clarify whether there were any differences in the characteristics of the secreted virus, we performed density gradient ultracentrifugation with the MA/JFH-1.2/R167G and MA/N3H+N5BX-JFH1/R167G viruses. The distributions of the HCV core protein and infectivity showed similar profiles (data not shown).

The differences between MA/JFH-1.2/R167G and MA/N3H+N5BX-JFH1/R167G are the NS2, NS3 protease domain (N3P), and NS4A to NS5A regions. Nucleotide variation(s) other than aa 167 in these regions of the MA strain may be associated with reduced virus assembly. We identified four additional cell culture-adaptive mutations, L814S (NS2), R1012G (NS2), T1106A (NS3), and V1951A (NS4B), which resulted from long-term culture of MA/N3H+N5BX-JFH1/R167G RNA-transfected cells. Consequently, cells transfected with MA/N3H+N5BX-JFH1/5am constructed by insertion of these four adaptive mutations into MA/N3H+N5BX-JFH1/R167G replicated and produced infectious virus as efficiently as MA/JFH-1.2/R167G RNA-transfected cells (Fig. 6).

This system is able to contribute to studies into the development of antiviral strategies. It has been reported that HCV genotype 2a was more sensitive to interferon therapy than HCV genotype 2b in a clinical study (20). To assess the interferon resistance of genotype 2b, a cell culture system with multiple genotype 2b strains is necessary. The previously reported replicable genotype 2b chimeric virus harbored only structural

regions of 2b strains (6, 27). The 2b/JFH-1 chimeric virus containing the region of the core protein to NS2 from the J8 strain (genotype 2b) and the region of NS3 to 3' X of JFH-1 was able to replicate and showed that there were no differences in interferon sensitivity among the JFH-1 chimeric viruses of other genotypes (6, 27). Another 2b/JFH-1 chimeric virus containing the regions of the core protein to NS2 (nt 342 to 2867) of a genotype 2b strain and of NS2 to 3' UTR (nt 2868) of JFH-1 has been reported (6, 27). The authors reported that their 2b/JFH-1 chimeric virus was more sensitive to interferon than JFH-1 (6, 27). We developed the genotype 2b HCV cell culture system with another HCV genotype 2b strain (MA). We identified a virus assembly-enhancing mutation in the core region, the minimal JFH-1 regions necessary for replication, and four additional adaptive mutations that enhance infectious virus production and demonstrated that MA harboring the five adaptive mutations and the 5' UTR and N3H and N5BX regions of JFH-1 (MA/N3H+N5BX-JFH1/5am) could replicate and produce infectious virus efficiently.

Using these novel genotype 2b chimeric viruses, we assessed interferon sensitivity. We found that MA/JFH-1.2/R167G chimeric virus and MA/N3H+N5BX-JFH1/5am virus were more sensitive to interferon than the JFH-1 virus (Fig. 7). Furthermore, we found that MA/N3H+N5BX-JFH1/5am was more sensitive to interferon than MA/JFH-1.2/R167G, indicating that the genetic variation(s) in the NS2, N3P, and NS4A to NS5A regions affect interferon sensitivity. Although genotype 2a viruses are more sensitive to interferon than genotype 2b viruses in clinical studies, JFH-1 displayed interferon resistance in our study.

These results suggest that the JFH-1 regions in the 2b/JFH-1 virus affect the interferon sensitivity of the chimeric virus. Moreover, it was reported that amino acid variations in E2, p7, NS2, and NS5A were associated with the response to peginterferon and ribavirin therapy in genotype 2b HCV infection (10). Therefore, our MA/JFH-1 chimeric virus harboring minimal regions from JFH-1 (MA/N3H+N5BX-JFH1/5am) is more suitable for assessing the characteristics of the MA strain than the MA/JFH-1 chimeric virus, which includes a nonstructural region from JFH-1 (MA/JFH-1.2/R167G). We showed here that replacement of the 5' UTR and N3H and N5BX regions in MA with those from JFH-1 is able to convert MA into a replicable virus. Using the same strategy, numerous HCV cell culture systems with various genotype 2b strains, as well as genotype 2a strains, may be available.

In conclusion, we established a novel HCV genotype 2b cell culture system using a chimeric genome in MA harboring minimal regions from JFH-1. This cell culture system using the chimeric genotype 2b virus will be useful for characterization of genotype 2b viruses and the development of antiviral strategies.

ACKNOWLEDGMENTS

We are grateful to Tetsuro Suzuki of Hamamatsu University School of Medicine for helpful comments and suggestions. Huh7.5.1 cells were kindly provided by Francis V. Chisari.

A.M. is partially supported by the Japan Health Sciences Foundation and Viral Hepatitis Research Foundation of Japan. This work was partially supported by Grants-in-Aid for Scientific Research from the Japan Society for the Promotion of Science, from the Ministry of Health, Labor and

Welfare of Japan, from the Ministry of Education, Culture, Sports, Science and Technology, from the National Institute of Biomedical Innovation, and by Research on Health Sciences Focusing on Drug Innovation from the Japan Health Sciences Foundation.

REFERENCES

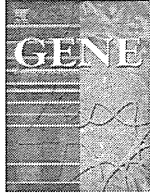
1. Akazawa D, et al. 2007. CD81 expression is important for the permissiveness of Huh7 cell clones for heterogeneous hepatitis C virus infection. *J. Virol.* 81:5036–5045.
2. Bartenschlager R, Lohmann V. 2000. Replication of hepatitis C virus. *J. Gen. Virol.* 81:1631–1648.
3. Boulant S, et al. 2006. Structural determinants that target the hepatitis C virus core protein to lipid droplets. *J. Biol. Chem.* 281:22236–22247.
4. Boulant S, Targett-Adams P, McLauchlan J. 2007. Disrupting the association of hepatitis C virus core protein with lipid droplets correlates with a loss in production of infectious virus. *J. Gen. Virol.* 88:2204–2213.
5. Choo QL, et al. 1989. Isolation of a cDNA clone derived from a blood-borne non-A, non-B viral hepatitis genome. *Science* 244:359–362.
6. Gottwein JM, et al. 2009. Development and characterization of hepatitis C virus genotype 1–7 cell culture systems: role of CD81 and scavenger receptor class B type I and effect of antiviral drugs. *Hepatology* 49:364–377.
7. Griffin S, et al. 2008. Genotype-dependent sensitivity of hepatitis C virus to inhibitors of the p7 ion channel. *Hepatology* 48:1779–1790.
8. Hope RG, McLauchlan J. 2000. Sequence motifs required for lipid droplet association and protein stability are unique to the hepatitis C virus core protein. *J. Gen. Virol.* 81:1913–1925.
9. Jensen TB, et al. 2008. Highly efficient JFH1-based cell-culture system for hepatitis C virus genotype 5a: failure of homologous neutralizing-antibody treatment to control infection. *J. Infect. Dis.* 198:1756–1765.
10. Kadokura M, et al. 2011. Analysis of the complete open reading frame of genotype 2b hepatitis C virus in association with the response to peginterferon and ribavirin therapy. *PLoS One* 6:e24514.
11. Kato T, et al. 2008. Hepatitis C virus JFH-1 strain infection in chimpanzees is associated with low pathogenicity and emergence of an adaptive mutation. *Hepatology* 48:732–740.
12. Kato T, et al. 2006. Cell culture and infection system for hepatitis C virus. *Nat. Protoc.* 1:2334–2339.
13. Kiyosawa K, et al. 1990. Interrelationship of blood transfusion, non-A, non-B hepatitis and hepatocellular carcinoma: analysis by detection of antibody to hepatitis C virus. *Hepatology* 12:671–675.
14. Lindenbach BD, et al. 2005. Complete replication of hepatitis C virus in cell culture. *Science* 309:623–626.
15. Lohmann V, et al. 1999. Replication of subgenomic hepatitis C virus RNAs in a hepatoma cell line. *Science* 285:110–113.
16. Masaki T, et al. 2008. Interaction of hepatitis C virus nonstructural protein 5A with core protein is critical for the production of infectious virus particles. *J. Virol.* 82:7964–7976.
17. Miyamoto M, Kato T, Date T, Mizokami M, Wakita T. 2006. Comparison between subgenomic replicons of hepatitis C virus genotypes 2a (JFH-1) and 1b (Con1 NK5.1). *Intervirology* 49:37–43.
18. Miyanari Y, et al. 2007. The lipid droplet is an important organelle for hepatitis C virus production. *Nat. Cell Biol.* 9:1089–1097.
19. Murakami K, Abe M, Kageyama T, Kamoshita N, Nomoto A. 2001. Down-regulation of translation driven by hepatitis C virus internal ribosomal entry site by the 3' untranslated region of RNA. *Arch. Virol.* 146:729–741.
20. Murakami T, et al. 1999. Mutations in nonstructural protein 5A gene and response to interferon in hepatitis C virus genotype 2 infection. *Hepatology* 30:1045–1053.
21. Murayama A, et al. 2007. The NS3 helicase and NS5B-to-3'X regions are important for efficient hepatitis C virus strain JFH-1 replication in Huh7 cells. *J. Virol.* 81:8030–8040.
22. Murayama A, et al. 2010. RNA polymerase activity and specific RNA structure are required for efficient HCV replication in cultured cells. *PLoS Pathog.* 6:e1000885.
23. Pietschmann T, et al. 2006. Construction and characterization of infectious intragenotypic and intergenotypic hepatitis C virus chimeras. *Proc. Natl. Acad. Sci. U. S. A.* 103:7408–7413.
24. Pietschmann T, et al. 2009. Production of infectious genotype 1b virus particles in cell culture and impairment by replication enhancing mutations. *PLoS Pathog.* 5:e1000475.
25. Scheel TK, et al. 2008. Development of JFH1-based cell culture systems

- for hepatitis C virus genotype 4a and evidence for cross-genotype neutralization. *Proc. Natl. Acad. Sci. U. S. A.* 105:997–1002.
26. Shavinskaya A, Boulant S, Penin F, McLauchlan J, Bartenschlager R. 2007. The lipid droplet binding domain of hepatitis C virus core protein is a major determinant for efficient virus assembly. *J. Biol. Chem.* 282: 37158–37169.
 27. Suda G, et al. 2010. IL-6-mediated intersubgenotypic variation of interferon sensitivity in hepatitis C virus genotype 2a/2b chimeric clones. *Virology* 407:80–90.
 28. Takeuchi T, et al. 1999. Real-time detection system for quantification of hepatitis C virus genome. *Gastroenterology* 116:636–642.
 29. Wakita T, et al. 2005. Production of infectious hepatitis C virus in tissue culture from a cloned viral genome. *Nat. Med.* 11:791–796.
 30. Yi M, Ma Y, Yates J, Lemon SM. 2007. Compensatory mutations in E1, p7, NS2, and NS3 enhance yields of cell culture-infectious intergenotypic chimeric hepatitis C virus. *J. Virol.* 81:629–638.
 31. Yi M, Villanueva RA, Thomas DL, Wakita T, Lemon SM. 2006. Production of infectious genotype 1a hepatitis C virus (Hutchinson strain) in cultured human hepatoma cells. *Proc. Natl. Acad. Sci. U. S. A.* 103:2310–2315.
 32. Zhong J, et al. 2005. Robust hepatitis C virus infection in vitro. *Proc. Natl. Acad. Sci. U. S. A.* 102:9294–9299.



Contents lists available at SciVerse ScienceDirect

Gene

journal homepage: www.elsevier.com/locate/gene

Detergent-induced activation of the hepatitis C virus genotype 1b RNA polymerase

Leiyun Weng^a, Michinori Kohara^b, Takaji Wakita^c, Kunitada Shimotohno^d, Tetsuya Toyoda^{a,b,e,*}

^a Unit of Viral Genome Regulation, Institut Pasteur of Shanghai, Key Laboratory of Molecular Virology & Immunology, Chinese Academy of Sciences, 411 Hefei Road, Shanghai 200025, PR China

^b Infectious Disease Regulation Project, Tokyo Metropolitan Institute of Medical Sciences, 1-6, Kamikitazawa 2-chome, Setagaya-ku, Tokyo 156-8506, Japan

^c Department of Virology II, National Institute of Health, 1-23-1 Toyama, Shinjuku, Tokyo 132-8640, Japan

^d Affiliated Research Institute, Chiba Institute of Technology, 2-17-1 Tsudamuna, Narashino, Chiba 275-0016, Japan

^e Choju Medical Institute, Fukushima Hospital, 19-4 Azanakayama, Noyori-cho, Toyohashi, Aichi 441-8124, Japan

ARTICLE INFO

Article history:

Accepted 18 January 2012

Available online 28 January 2012

Keywords:

HCV
NS5B
RNA polymerase
In vitro transcription
Triton X-100
Oligomer

ABSTRACT

Recently, we found that sphingomyelin bound and activated hepatitis C virus (HCV) 1b RNA polymerase (RdRp), thereby recruiting the HCV replication complex into lipid raft structures. Detergents are commonly used for resolving lipids and purifying proteins, including HCV RdRp. Here, we tested the effect of detergents on HCV RdRp activity in vitro and found that non-ionic (Triton X-100, NP-40, Tween 20, Tween 80, and Brij 35) andwitterionic (CHAPS) detergents activated HCV 1b RdRps by 8–16.6 folds, but did not affect 1a or 2a RdRps. The maximum effect of these detergents was observed at around their critical micelle concentrations. On the other hand, ionic detergents (SDS and DOC) completely inactivated polymerase activity at 0.01%. In the presence of Triton X-100, HCV 1b RdRp did not form oligomers, but recruited more template RNA and increased the speed of polymerization. Comparison of polymerase and RNA-binding activity between JFH1 RdRp and Triton X-100-activated 1b RdRp indicated that monomer RdRp showed high activity because JFH1 RdRp was a monomer in physiological conditions of transcription. Besides, 502H plays a key role on oligomerization of 1b RdRp, while 2a RdRps which have the amino acid S at position 502 are monomers. This oligomer formed by 502H was disrupted both by high salt and Triton X-100. On the contrary, HCV 1b RdRp completely lost fidelity in the presence of 0.02% Triton X-100, which suggests that caution should be exercised while using Triton X-100 in anti-HCV RdRp drug screening tests.

© 2012 Elsevier B.V. All rights reserved.

1. Introduction

Hepatitis C virus (HCV) belongs to the family *Flaviviridae* and has a positive-stranded RNA genome (Lemon et al., 2007). HCV chronically infects more than 130 million people worldwide (Wasley and Alter, 2000), and infection often induces liver cirrhosis and/or hepatocellular carcinoma (Kiyosawa et al., 1990; Saito et al., 1990). The 9.6-kb-long HCV RNA genome has a long open reading frame encoding a polyprotein of approximately 3,010 amino acids, which is processed into at least 10 viral proteins (NH₂-C-E1-E2-p7-NS2-NS3-NS4A-NS4B-NS5A-NS5B-COOH) by host and viral proteases (Grakoui et al., 1993; Hijikata et al., 1993). The 5′-untranslated region (UTR) contains

the internal ribosome entry site (IRES) (Tsukiyama-Kohara et al., 1992). The 3′-UTR contains a poly pyrimidine “U/C” tract, a variable region, and 98-base X-region (Tanaka et al., 1996).

HCV RNA replication depends on the association between the viral protein and raft membranes (Shi et al., 2003; Aizaki et al., 2004), where NS5B RNA polymerase (RdRp) localizes by binding to sphingomyelin (Sakamoto et al., 2005). HCV RdRp is a key enzyme involved in the transcription and replication of the viral genome, and an important target of antivirals. Recently, we found that sphingomyelin bound to and activated HCV 1b RdRp, thereby recruiting the HCV replication complex into lipid raft structures (Weng et al., 2010).

Detergents are commonly used for solubilizing proteins from the lipid-containing components. Some restriction enzymes, reverse transcriptases, and Taq polymerases are stabilized by Triton X-100 or NP-40 (Weyant et al., 1990), while some other polymerases are activated by detergents (Thompson et al., 1972; Wu and Cetta, 1975; Hirschman et al., 1978). Triton X-100 is used for purification of HCV RdRp (Weng et al., 2009). Oligomerization of HCV RdRp is important for its activity (Qin et al., 2002; Clemente-Casares et al., 2011). We have developed an in vitro HCV de novo transcription system by using soluble RdRp and the complementary sequence of the 5′-HCV

Abbreviations: CHAPS, 3-[(3-cholanidopropyl)dimethylammonio]-1-propanesulfonate; CMC, critical micelle concentration; DOC, sodium deoxycholate; HCV, hepatitis C virus; IRES, internal ribosome entry site; KGLu, monopotassium glutamate; PMSF, phenylmethanesulfonyl fluoride; RdRp, RNA polymerase; SDS, sodium dodecyl sulfate; TNTase, terminal nucleotidyl transferase; UTR, untranslated region; nOG, octyl-β-glucoside.

* Corresponding author at: Choju Medical Institute, Fukushima Hospital, 19-4 Azanakayama, Noyori-cho, Toyohashi, Aichi 441-8124, Japan. Tel.: +81 532 46 7511; fax: +81 532 46 8940.

E-mail address: toyoda_tetsuya@yahoo.co.jp (T. Toyoda).

genome RNA (SL12-1S template) (Kashiwagi et al., 2002a; Kashiwagi et al., 2002b; Weng et al., 2009; Murayama et al., 2010; Weng et al., 2010). In this paper, we analyzed the effect of detergents on the activity and oligomerization of HCV RdRp, and found that non-ionic (Triton X-100, NP-40, Tween 20, Tween 80, and Brij 35) and twitterionic (3-[(3-cholanidopropyl)dimethylammonio]-1-propanesulfonate [CHAPS]) detergents activated HCV 1b RdRp. In addition, we analyzed the mechanism of RdRp activation by detergents and the relationship between RdRp oligomerization and its activity.

2. Materials and methods

2.1. Mutant HCV RdRp

The H502S mutation of HCR6 (1b) RdRp and the S502H mutation of JFH1 (2a) were introduced using an in vitro mutagenesis kit (Stratagene). Oligonucleotide sequence information is available upon request.

2.2. Purification of HCV RdRp from bacteria

HCV HCR6wt (1b) (Weng et al., 2009), NN (1b) (Watashi et al., 2005), Con1 (1b) (Binder et al., 2007), JFH1wt (2a) (Weng et al., 2009), J6CF (2a) (Murayama et al., 2007), H77 (1a) (Blight et al., 2003), RMT (1a), HCR6 (1b) H502S, and JFH1 (2a) H502S RdRps with a C-terminal 21-amino acid deletion were purified from bacteria as previously described with some modifications (Weng et al., 2009, 2010; Murayama et al., 2010). Briefly, HCV RdRps were eluted from Ni-NTA agarose (Qiagen) with 20 mM Tris-HCl (pH 8.0), 500 mM NaCl, 0.1% Triton X-100, 0.1% 2-mercaptoethanol, and 1 mM phenylmethanesulfonyl fluoride (PMSF) containing 250 mM imidazole after the column was washed with 5 mM imidazole. HCV RdRps were further purified through a Superdex 200 pg column (GE Healthcare) in 20 mM Tris-HCl (pH 8.0), 500 mM NaCl, 1 mM EDTA, 5 mM DTT, 10% glycerol, and 1 mM PMSF to remove contaminating nucleic acids (Fig. S1). The purified HCV RdRps were stored at -80°C .

2.3. De novo HCV RdRp assay

HCV RdRp assay in the absence of primers was performed as described previously (Weng et al., 2009; Murayama et al., 2010). Briefly, following a 30-min pre-incubation period without ATP, CTP, or UTP, 100 nM HCV RdRp were incubated in 50 mM Tris-HCl (pH 8.0), 200 mM monopotassium glutamate (KGlU), 3.5 mM MnCl_2 , 1 mM DTT, 0.5 mM GTP, 50 μM ATP, 50 μM CTP, 5 μM [α - ^{32}P]UTP, 200 nM 184-nt model RNA template (SL12-1S) (Kashiwagi et al., 2002a; Weng et al., 2009; Murayama et al., 2010), 100 U/ml human placental RNase inhibitor, and the indicated amount of detergent at 29°C for 90 min. [^{32}P]RNA products were separated in a 6% polyacrylamide gel containing 8 M urea. The resulting autoradiograph was analyzed with a Typhoon Trio Plus image analyzer (GE Healthcare) for the radio activity of 184-nt transcription products.

2.4. Kinetic analysis of HCV RdRp with and without Triton X-100

Kinetic analysis (measurement of K_m and V_{max}) was performed as previously published with and without 0.02% Triton X-100 (Kashiwagi et al., 2002b; Weng et al., 2009). For K_m and V_{max} of ATP, HCV RdRp was incubated in 50, 25, 10, 8, 5, 3, or 1 μM of ATP, 50 μM CTP, 0.5 mM GTP, 5 μM [α - ^{32}P]UTP after preincubation in 0.5 mM GTP with and without 0.02% Triton X-100 at 29°C for 60 min. For K_m and V_{max} of CTP, 50, 25, 10, 8, 5, 3, or 1 μM of CTP, 50 μM ATP, 0.5 mM GTP, and 5 μM [α - ^{32}P]UTP, and for K_m and V_{max} of UTP, 50, 25, 10, 8, 5, 3, or 1 μM of UTP, 50 μM ATP, 0.5 mM

GTP, 5 μM [α - ^{32}P]CTP were used, respectively. For K_m and V_{max} of GTP, HCV RdRp was incubated in 500, 250, 100, 50, 25, 10, or 5 μM of GTP, 50 μM ATP, 50 μM CTP, 5 μM [α - ^{32}P]UTP with and without 0.02% Triton X-100 without GTP preincubation.

2.5. Terminal nucleotidyl transferase (TNTase) assay

TNTase assay was performed with the heat denatured 5'-[^{32}P]sym/sub (5'-GAUCGGGCCCGAUC-3') (Arnold and Cameron, 2000) with 0.5 mM GTP, 50 μM ATP, 50 μM CTP, and 50 μM UTP, and sym/sub with 0.5 mM GTP, 50 μM ATP, 50 μM CTP, and 5 μM [α - ^{32}P]UTP in the same experimental conditions as the above-described transcription assay (Hong et al., 2001). [^{32}P]RNA products were separated in a 15% polyacrylamide gel containing 8 M urea.

2.6. RNA filter-binding assay

RNA filter-binding assays were performed as previously described (Weng et al., 2009). Briefly, 100 nM of HCV RdRp and 100 nM [^{32}P]RNA template (SL12-1S) were incubated with the indicated amount of detergent in 25 μl of 50 mM Tris-HCl (pH 7.5), 200 mM KGlU, 3.5 mM MnCl_2 , and 1 mM DTT at 29°C for 30 min. After incubation, the solutions were diluted with 0.5 ml TE and filtered through nitrocellulose membranes (0.45 μm ; Millipore). The filter was washed 5 times with TE, and the bound radioisotope was analyzed using the Typhoon Trio Plus image analyzer after being dried.

2.7. Western blot

Western blot analysis using a rabbit anti-HCV RdRp antibody was performed, as described previously (Kashiwagi et al., 2002b).

2.8. Gel filtration

The purified HCR6 (1b), J6CF (2a), and JFH1 (2a) RdRps (50 pmol) were applied on a Superdex 200 pg column in 50 mM Tris-HCl (pH 7.5), 200 mM KGlU or 150 mM NaCl, 3.5 mM MnCl_2 , 1 mM DTT, and 0.2% glycerol with or without 0.1% Triton X-100.

2.9. Reagents

PMSF, Triton X-100, Tween 20, Tween 80, NP-40, Brij 35, octyl- β -glucoside (nOG), CHAPS, sodium deoxycholate (DOC), and sodium dodecyl sulfate (SDS) were obtained from Amresco; nucleotides were purchased from GE Healthcare; [α - ^{32}P]UTP, [α - ^{32}P]ATP, [α - ^{32}P]GTP, [α - ^{32}P]CTP, and [γ - ^{32}P]ATP were from New England Nuclear.

2.10. Statistical analysis

Significant differences were determined using the Student's *t*-test.

3. Results

3.1. Effect of detergents on primer-independent HCV RdRp activity

First, we examined the effect of detergents on the primer-independent HCV RdRp activity in vitro (Fig. 1). HCR6 (1b) RdRpwt was activated by all the detergents tests, except octyl- β -glucoside (nOG), but JFH1 (2a) RdRpwt was not. The activation curves of HCR6 (1b) RdRpwt by these detergents plateaued at certain concentrations: 0.002 or 0.004% Triton X-100, 0.001% NP-40, 0.005% Tween 20, 0.001% Tween 80, 0.001% Brij 35, and 0.1% CHAPS. HCR6 (1b) RdRp activity decreased at concentrations greater than 1% Triton X-100, and 30% Triton X-100 completely inhibited HCR6 (1b) RdRpwt activity (Fig. 1A, right panel). With an activation ratio of about 2 at 0.1%, nOG weakly activated HCR6 (1b) RdRpwt. At 0.5% nOG, the

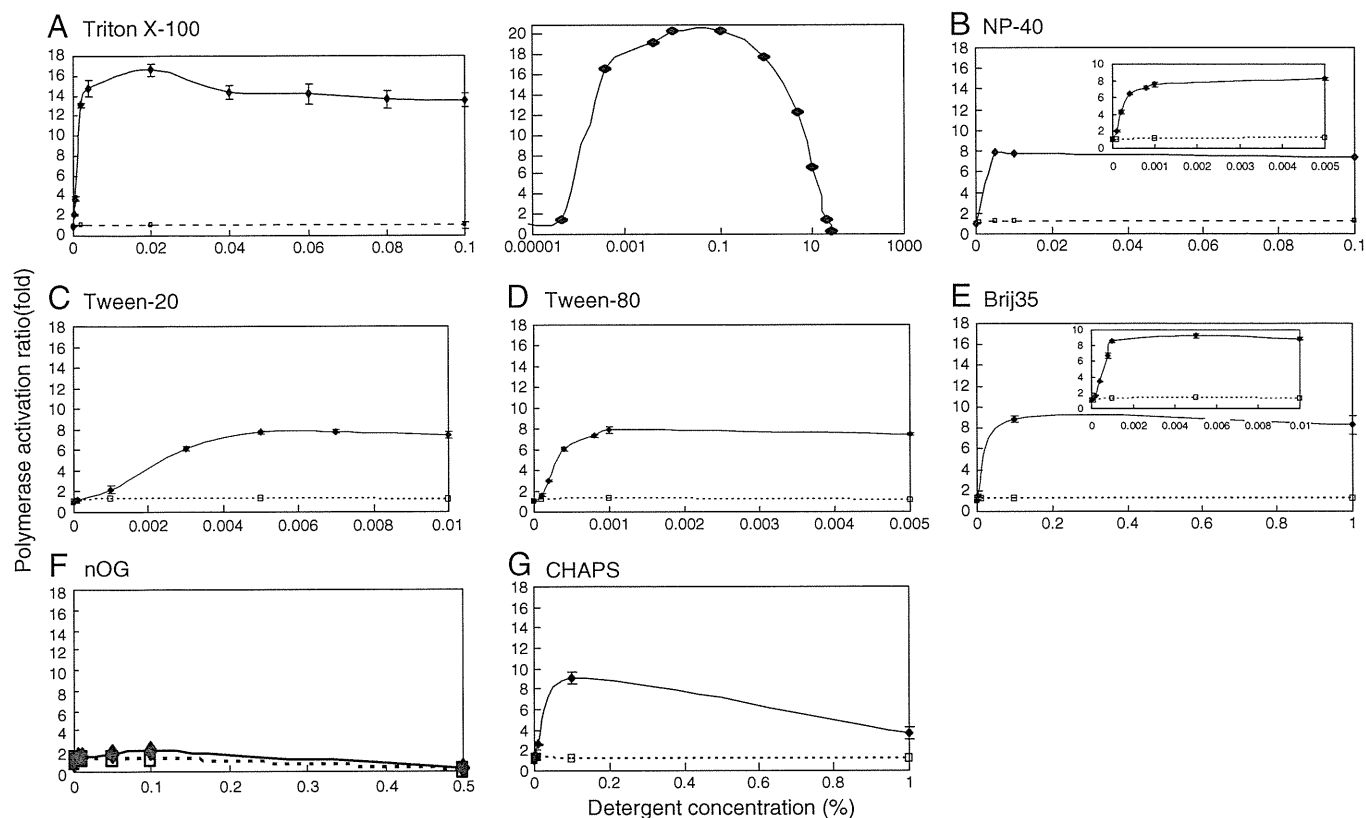


Fig. 1. The effect of detergents on HCV HCR6 and JFH1 RNA polymerases. Wild-type HCR6 (1b) and JFH1 (2a) RdRps were assayed with 0.000004, 0.00004, 0.0004, 0.004, 0.01, 0.02, 0.04, 0.06, 0.08, and 0.1% Triton X-100 (A, left panel); 0.0001, 0.0002, 0.0004, 0.0008, 0.001, 0.005, 0.1, and 0.5% NP-40 (B); 0.0001, 0.001, 0.003, 0.005, 0.007, and 0.01% Tween 20 (C); 0.0001, 0.0002, 0.0004, 0.0008, 0.001, and 0.005% Tween 80 (D); 0.0001, 0.0002, 0.0004, 0.0008, 0.001, 0.005, 0.01, 0.1, and 1% Brij 35 (E); 0.001, 0.005, 0.01, 0.05, and 0.1% nOG (F); or 0.0001, 0.001, 0.005, 0.01, 0.1, 0.1, and 1% CHAPS (G). The effect of high concentration of Triton X-100 on HCR6 (1b) RdRpwt is shown in A (right panel). Inset: Polymerase activation ratio at a lower concentration of NP-40 (B), and Brij 35 (E). Mean and standard deviation (error bar) of the polymerase activation ratio were calculated from 3 independent experiments. The solid line indicates the activation ratio of HCR6 (1b) RdRpwt, and the broken line indicates that of JFH1 (2a) RdRpwt.

activation ratio of HCR6 (1b) RdRpwt was 0.3. At 1% of CHAPS, the activity of HCR6 (1b) RdRpwt was increased by 3.6 folds. The detergent concentration that most activated HCR6 (1b) RdRpwt was approximate to the critical micelle concentration (CMC; Table 1).

When the activation ratios of detergents on HCR6 (1b) RdRpwt were compared, that of Triton X-100 was the highest (Fig. 2, Table 1). Other non-ionic detergents and CHAPS activated HCR6 (1b) RdRpwt to an extent equal to about half of Triton X-100 activation. Although a non-ionic detergent, nOG barely activated HCR6 (1b) RdRpwt.

Because 0.02% Triton X-100 maximally activated HCR6 (1b) RdRpwt, we compared its activation effect on other HCV RdRps (Fig. 3, Table 2). JFH1 (2a) RdRpwt showed the strongest RdRp activity, which is in accordance with previous reports (Weng et al., 2009;

Murayama et al., 2010; Schmitt et al., 2011). The RdRp activities of 1b HCR6 and NN activated by Triton X-100 were similar to that of JFH1 RdRpwt in the absence of detergents (Fig. 3B), whereas the RdRp activity of Triton X-100-activated 1b Con1 was about half of that of wild-type JFH1. Neither 1a nor 2a RdRps were activated by Triton X-100.

3.2. RNA template binding with Triton X-100

Next, we compared the template RNA-binding activity of 1a, 1b, and 2a RdRps in the presence of Triton X-100 by using the [³²P] SL12-1S model RNA template (Kashiwagi et al., 2002a; Weng et al., 2009, 2010; Murayama et al., 2010) in order to examine the transcription steps activated by Triton X-100 (Fig. 4, Table 2). Template RNA binding was the first step of transcription. The RNA-binding activity of JFH1 RdRpwt was the highest without Triton X-100 (data not shown) (Weng et al., 2009). Different from RdRp activity, the RNA-binding activity of all HCV RdRps was somehow activated by 0.02% Triton X-100. The RNA-binding activity of 1b RdRps was increased by 7–10 folds with Triton X-100.

3.3. Gel filtration of 1b and 2a RdRps

Proteins are generally soluble in detergents. Because HCR6 (1b) RdRpwt showed similar polymerase activity with Triton X-100 as JFH1 (2a) RdRpwt without Triton X-100, we compared the oligomerization state of these RdRps. The oligomerization state of HCR6 (1b) and JFH1 (2a) RdRps under transcription (physiological) conditions (200 mM KClu or 150 mM NaCl) was analyzed by gel filtration on

Table 1
CMC and HCV HCR6 (1b) RdRpwt activation ratio of different detergents.

Detergent	CMC ^a in H ₂ O (%)	Minimal concentration of maximal activation (%)	Maximal activation (folds) ^b
Triton X-100	0.0155	0.02	16.6 ± 0.56
NP-40	0.0179	0.005	8.3 ± 0.18
Tween 20	0.0074	0.007	7.8 ± 0.21
Tween 80	0.0016	0.001	8.0 ± 0.22
Brij 35	0.1103	0.1	9.2 ± 0.34
nOG	0.672–0.730	0.1	2.1 ± 0.35
CHAPS	0.492–0.615	0.1	9.1 ± 0.60

^a Modified from "TECHNICAL RESOURCE" (Pierce).

^b Calculated from Fig. 2.

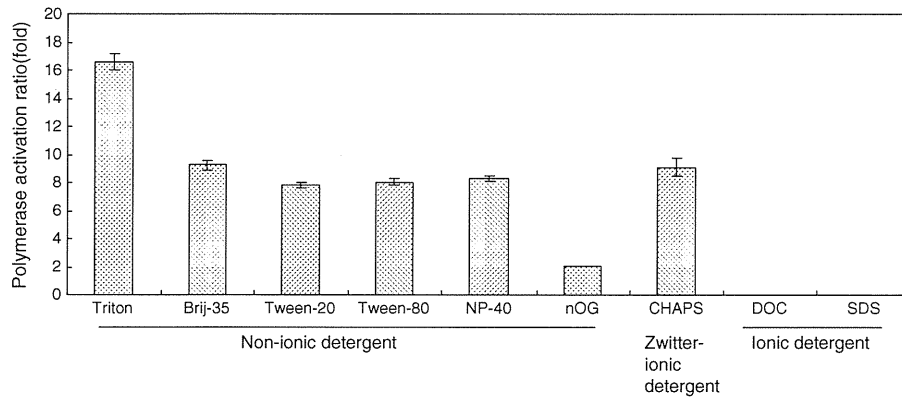


Fig. 2. Activation effect of HCV HCR6 polymerase with detergents at CMC. HCV HCR6 (1b) RdRpwt was assayed at CMC in the presence of Triton X-100 (0.02%), Brij 35 (0.1%), Tween 20 (0.007%), Tween 80 (0.001%), NP40 (0.005%), nOG (0.1%), CHAPS (0.1%), DOC (0.001%), and SDS (0.001%). The activation ratio (fold) is indicated in Table 2. Mean and standard deviation (error bar) of the polymerase activity relative to that without detergent were calculated from 3 independent experiments.

Superdex 200 (Figs. 5 and 6). HCR6 (1b) RdRpwt was eluted from the void volume fraction to the 158-kDa fraction without Triton X-100 (Fig. 5A), which meant that HCR6 (1b) RdRpwt formed random oligomers. It was eluted in the 38-kDa fraction with 0.1% Triton X-100 (Fig. 5B), which indicated that it was smaller than its monomer gel filtration size (Fig. S1D). However, JFH1 (2a) RdRpwt was eluted in the slightly larger fraction (80 kDa) than other HCV RdRps with or without Triton X-100, which indicated the monomer size (Figs. 5C and D, S1F). From the gel filtration and transcription data of HCR6 (1b) RdRpwt and JFH1 (2a) RdRpwt, it was concluded that Triton X-100 dispersed HCR6 (1b) RdRpwt, and that the higher-ordered

oligomers of HCR6 (1b) RdRpwt were inactive. Triton X-100 might also affect the interaction between HCR6 (1b) RdRpwt and Superdex200 gel matrix because it was eluted in the smaller molecular weight fractions with Triton X-100 than the monomer gel-filtration size in 0.5 M NaCl (76 kDa, Fig. S1D). Western blot analysis indicated that these RdRp were not degraded (Figs. 5A and B, inset).

Qin et al. found that amino acids 18E and 502H interacted with each other to form the HCV 1b RdRp oligomer/dimer (Qin et al., 2002). Only 2a RdRps harbor the amino acid S at position 502, contrary to other genotype forms of RdRps, which harbor the amino acid H at that same position (Table S1). Therefore, we first examined

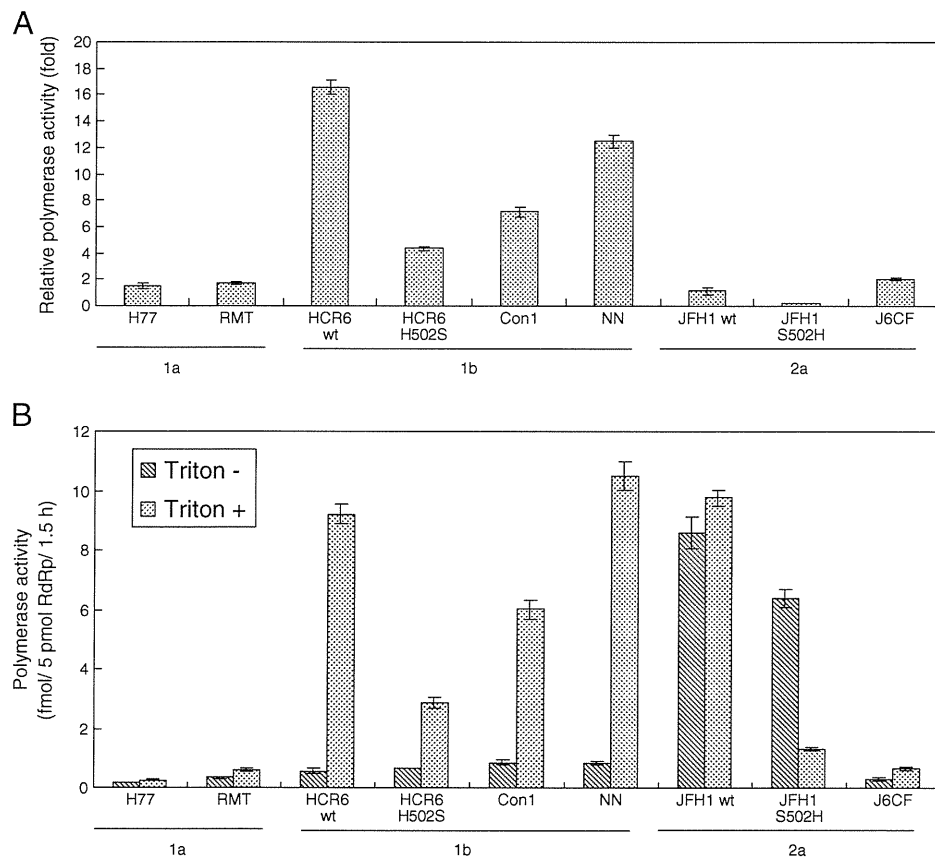


Fig. 3. Effect of 0.02% Triton X-100 on various HCV RNA polymerases. HCV H77 (1a), RMT (1a), HCR6 (1b) wt and H502S, NN (1b), Con1 (1b), JFH1 (2a) wt and S502H, and J6CF (2a) RdRps were assayed in the presence or absence of Triton X-100. A: Activation ratio (fold) of RNA polymerase activity. B: Polymerase activity (fmol of NMP/5 pmol RdRp/1.5 h) in the presence or absence of Triton X-100. Mean and standard deviation (error bar) of the polymerase activity were calculated from 3 independent experiments.

Table 2
Relative activation ratio of HCV RdRp by Triton X-100.

Genotype	1a		1b			2a	
	H77	RMT	HCR6	Con1	NN	JFH1	J6CF
Polymerase activity (folds) ^a	1.5 ± 0.17	1.7 ± 0.11	16.6 ± 0.56	7.1 ± 0.38	12.5 ± 0.48	1.1 ± 0.28	2.0 ± 0.12
RNA template-binding activity (folds) ^b	3.8 ± 0.11	3.9 ± 0.18	9.6 ± 0.39	7.9 ± 0.41	6.9 ± 0.16	2.2 ± 0.14	3.4 ± 0.21

^a Activation ratio of polymerase activity was calculated on the basis of the data represented in Fig. 3A.

^b Activation ratio of RNA template-binding activity was calculated on the basis of the data represented in Fig. 4A.

another 2a RdRp, J6CF (2a) RdRp, by gel filtration (Fig. 5E). J6CF (2a) RdRp was also eluted as a monomer in 150 mM NaCl buffer without Triton X-100. These gel filtration data was in agreement with the intermolecular interaction and random oligomerization of HCV RdRp caused by 18E and 502E (Qin et al., 2002). Amino acid 18E is shared by HCV RdRps of all 6 genotypes (Table S1) (Clemente-Casares et al., 2011). Therefore, in order to confirm the importance of 502H for oligomerization of HCV RdRp, S502H and H502S mutations were introduced into JFH1 (2a) and HCR6 (1b) RdRps, respectively, and analyzed by gel filtration (Fig. 6). JFH1 (2a) RdRpS502H formed oligomers, and HCR6 (1b) RdRpH502S was eluted in the 15-kDa fraction, which was smaller than its monomeric gel-filtration size. JFH1 (2a) RdRpS502H was eluted around the 50-kDa position with Triton X-100. The RdRp dimers (Qin et al., 2002) were not found in any of our gel filtration profiles. Western blot analysis indicated that the proteins were not degraded (Fig. 6, inset).

The effect of these mutations in RdRp and RNA template-binding activity with and without Triton X-100 was examined (Figs. 3 and 4). JFH1 (2a) RdRpS502H RdRp activity was lower than that of the wild-type in the absence of Triton X-100. Different from the Triton X-100 activation effect on HCR6 (1b) RdRpwt, JFH1 (2a) RdRpS502H RdRp activity decreased, while its RNA template binding increased, in the presence of Triton X-100. HCR6 (1b) RdRpH502S RdRp activity was similar to that of the wild-type, but less activated by Triton X-100 than by the wild-type. RNA template-binding activity of HCR6 (1b) RdRpH502S was activated 2.3 times by Triton X-100.

The 502 mutation data indicated that 502H is important for oligomerization of 1b RdRp molecules in the transcription (physiological salt) condition. Triton X-100 prevented the oligomerization of 1b RdRps by 502H. Moreover, For HCR6 (1b) RdRpwt, the 38-kDa gel filtration molecules (Fig. 5B), which might correspond to the monomer, were more active than the oligomer molecules.

3.4. Fidelity of HCV RdRp with Triton X-100

Finally, we aimed to calculate the kinetic constants (K_m and V_{max}) of HCR6 (1b) RdRp in the presence of 0.02% Triton X-100 because the activation ratio of the polymerase activity was higher than that of RNA binding of HCR6 (1b) RdRp. When nucleotide concentration was low, the amount of product without Triton X-100 decreased; this data can be used to draw Lineweaver–Burk plot (Weng et al., 2009). However, with Triton X-100, the product amount did not decrease according to the decrease of each nucleotide (Fig. 7A). Moreover, each of the nucleotide substrates was removed from the standard HCV in vitro transcription condition (Fig. 7B). Although ATP, CTP or UTP were removed from the reaction buffer, HCV HCR6 (1b) RdRp transcribed the same 184-nt products with Triton X-100, which disappeared without Triton X-100. When GTP was removed, no products were observed with or without Triton X-100 because HCV RdRp required GTP for its structure (Bressanelli et al., 2002). These kinetic experiments indicated that HCV HCR6 (1b) RdRp completely lost fidelity with Triton X-100.

Terminal nucleotidyl transferase (TNTase) activity has been sometimes detected in HCV 1b RdRp preparations (Behrens et al., 1996; Ranjith-Kumar et al., 2001; Ranjith-Kumar et al., 2004; Vo et al., 2004). TNTase activity was not detected in our system, in which the model RNA template contains a CCC-3' at the 3'-end (Kashiwagi et al., 2002b; Weng et al., 2009). Nevertheless, we examined whether TNTase activity was detected with Triton X-100 using sym/sub, which has GpG-primed transcription activity, but we failed to observe any de novo initiation activity (Hong et al., 2001). No mobility shift was shown by 5'-[³²P]sym/sub or sym/sub incubated with [³²P]UTP on polyacrylamide gel electrophoresis (PAGE) (Figs. 7C and D), indicating that no TNTase activity was detected in our system with or without Triton X-100.

Apparent K_m and V_{max} of HCR6 (1b) RdRp with Triton X-100 for GTP was $303 \pm 15.1 \mu\text{M}$ and $6.21 \pm 0.225/\text{min}$, respectively (Fig. S3).

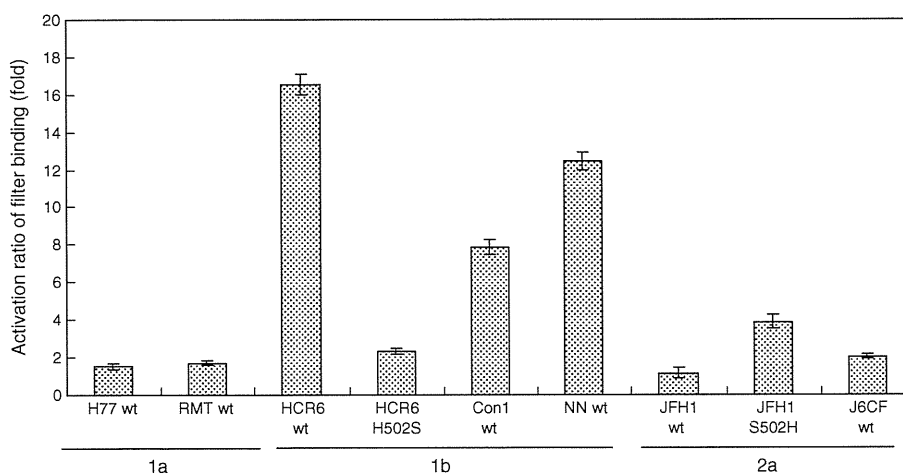


Fig. 4. Effect of 0.02% Triton X-100 on the RNA template-binding activity of HCV RNA polymerases. One hundred nanomolars each of HCV H77 (1a), RMT (1a), HCR6 (1b), NN (1b), Con1 (1b), JFH1 (2a), and J6CF (2a) RdRps with [³²P]RNA templates (SL12-15) were filtered through nitrocellulose membranes after incubation with or without Triton X-100. Mean and standard deviation (error bar) of the RNA filter binding activation (folds) were calculated from 3 independent experiments.

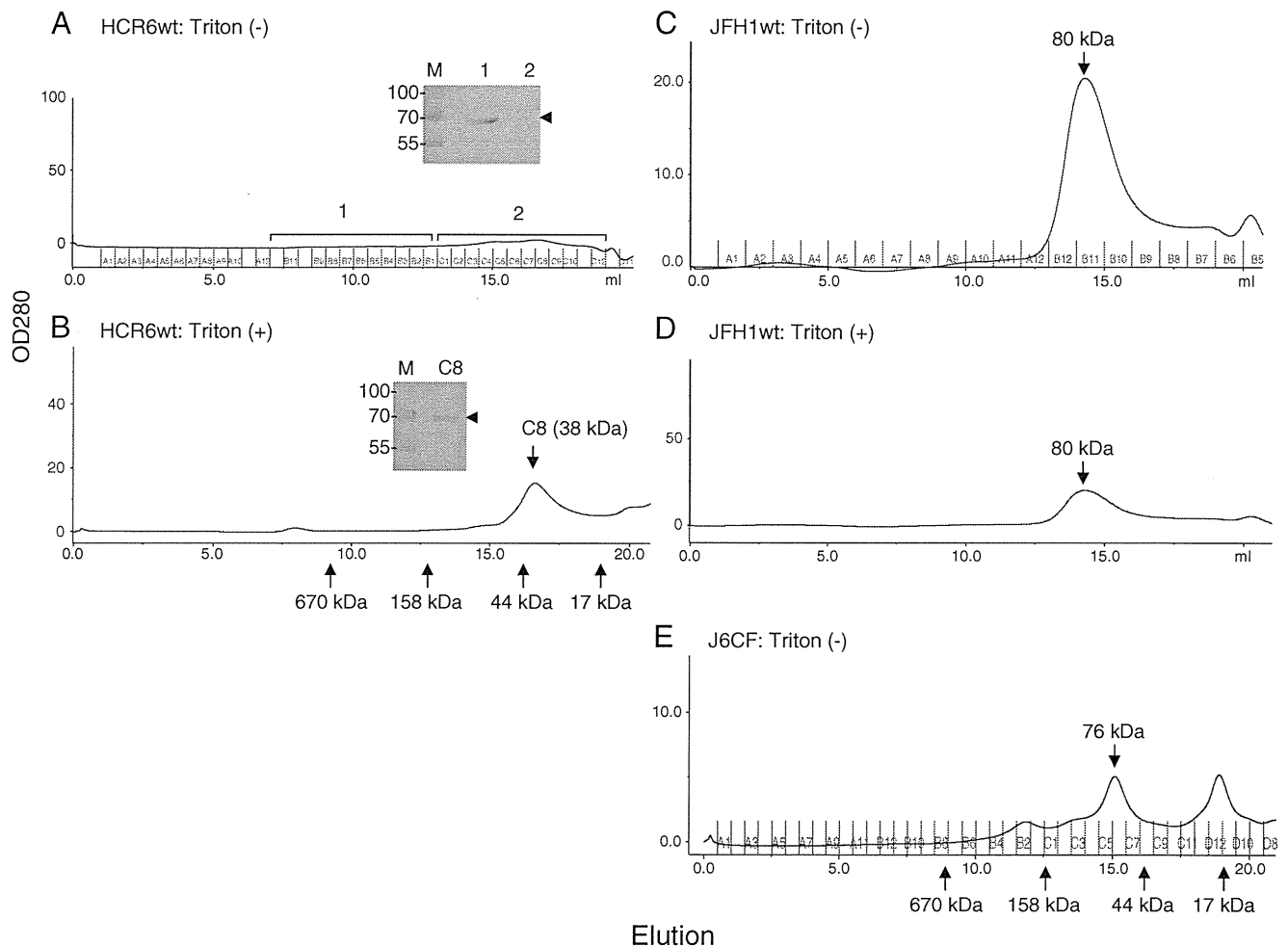


Fig. 5. Superdex 200 gel filtration of HCV HCR6 (1b), JFH1 (2a), and J6CF (2a) wild-type RNA polymerase with or without 0.1% Triton X-100. HCV HCR6 (1b) RdRpwt was applied on Superdex 200 gel filtration columns in 50 mM Tris-HCl (pH 7.5), 150 mM NaCl, 3.5 mM MnCl₂, 1 mM DTT, and 0.2% glycerol without (A) or with 0.1% Triton X-100 (B). HCV JFH1 (2a) RdRpwt was applied without (C) or with 0.1% Triton X-100 (D), and J6CF (2a) RdRp was applied without Triton X-100 (E) on the same columns. The elution position of the standard molecular weight markers is indicated below the graph. The molecular weight of the peak fraction is indicated in each graph. Inset in A: The fractions of the void volume–158 kDa (1) and those of lower molecular weight fractions (2) of HCR6 (1b) RdRpwt gel filtration without Triton X-100 were precipitated with TCA and analyzed by western blot. Inset in B: Fraction C8 of HCR6 (1b) RdRpwt with Triton X-100 was precipitated with TCA and analyzed by western blot. The position of HCR6 (1b) RdRpwt is indicated by an arrowhead. The position of the pre-stained size marker is indicated on the left side of the blots.

K_m and V_{max} of HCR6 (1b) RdRp without Triton X-100 for GTP was calculated as $54.7 \pm 3.67 \mu\text{M}$ and $2.52 \pm 0.108/\text{min}$, respectively (Weng et al., 2009).

4. Discussion

Non-ionic (Triton X-100, NP-40, Tween 20, Tween 80, and Brij 35) and twitterionic (CHAPS) detergents activated HCV 1b RdRp by 7.2–16.6 folds when used at their CMC, but did not affect 1a or 2a RdRps (Figs. 1–3, Table 2). In turn, ionic detergents (SDS and DOC) completely inactivated polymerase activity at 0.01%. CMC is the minimum concentration at which a detergent forms micelles; above that concentration, a detergent exists as a large molecular weight complex. The CMC signifies the strength at which a detergent binds to proteins, i.e., low values indicate strong binding, whereas high values indicate weak binding. It is also an indication of the hydrophilicity of a detergent. Triton X-100, NP-40, and Brij 35 at CMC activated Moloney leukemia virus reverse transcriptase by interacting with the hydrophobic domain (Thompson et al., 1972). The activation mechanism of HCV RdRp by these detergents may be similar. However, the detergent interaction domain of HCV RdRp remains to be identified.

Triton X-100 is commonly used for purification of HCV RdRp from the bacteria and insect cells expressing this protein (Lohmann et al.,

1997; Luo et al., 2000; Cramer et al., 2006; Weng et al., 2009). HCV 1b RdRp without the C-terminal hydrophobic region expressed in bacteria formed a large molecule complex in 0.1% Triton X-100 or 0.5% CHAPS with a low-salt buffer (<50 mM NaCl) (Qin et al., 2002; Wang et al., 2002). Under low-salt conditions, HCV RdRp was gel filtered in void volume as a complex with contaminating nucleic acids, because HCV RdRp binds to RNA during purification without high-salt (0.5 M NaCl) stripping (Figs. S1 and S2). Therefore, the presence of HCV 1b RdRp in the void volume fraction of gel filtration by Wang et al. (Wang et al., 2002) could rather represent the complex of HCV RdRp with contaminating nucleic acids. Nevertheless, they also found monomers of HCV 1b RdRp in the gel filtration buffer containing 0.5% CHAPS, which activated polymerase activity (Fig. 1G). Detection of the monomeric HCV 1b RdRps by gel filtration in a buffer containing Triton X-100 and CHAPS has also been reported by other groups (Qin et al., 2002; Wang et al., 2002). HCR6 (1b) RdRpwt formed oligomers in physiological conditions without Triton X-100. In the presence of Triton X-100, HCR6 (1b) RdRpwt was eluted as the monomer which gel-filtration size was smaller than its size in 0.5 M NaCl (Fig. S1D) or calculated from its amino acid composition (64 kDa). HCV 2a (JFH1 and J6CF) RdRps formed a monomer in the same buffer without Triton X-100. Gel filtration analysis of 502 mutants of JFH1 (2a) and HCR6 (1b) RdRps have confirmed that 502H

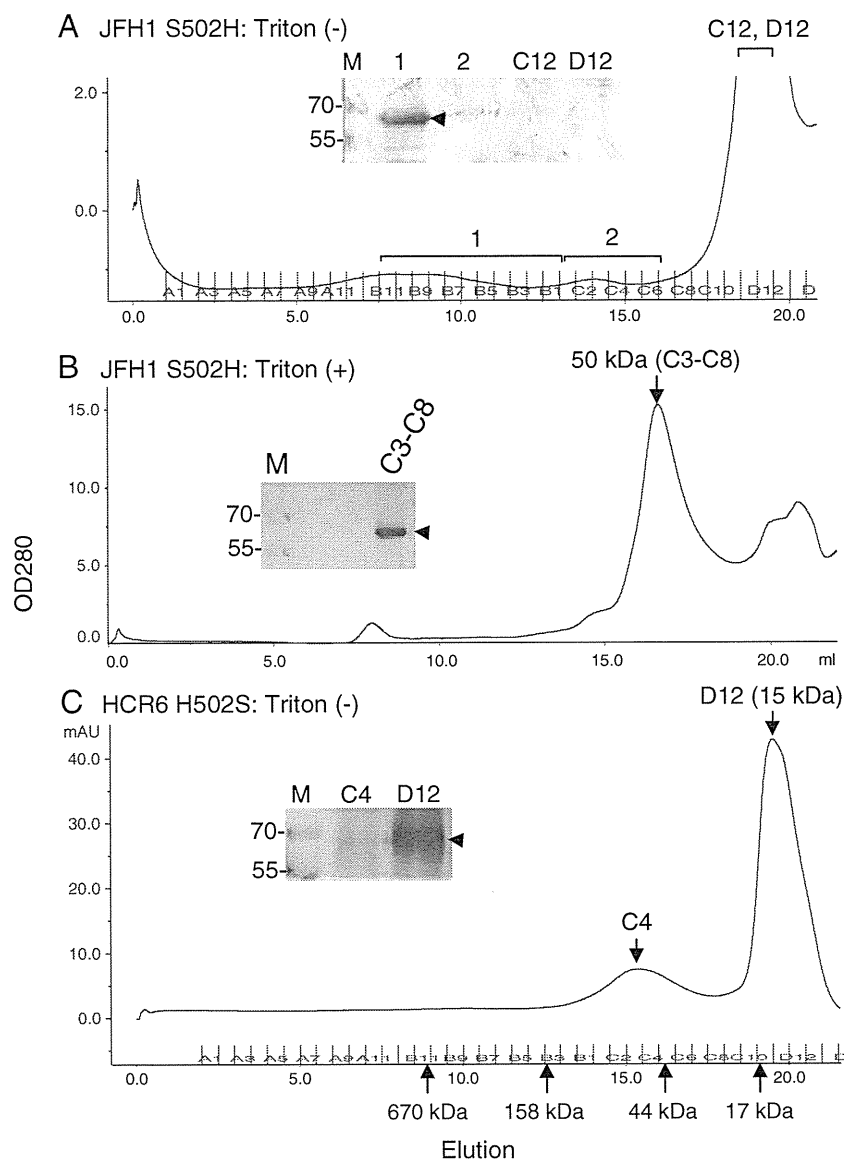


Fig. 6. Superdex 200 gel filtration of HCV JFH1 (2a) and HCR6 (1b) 502 mutant RNA polymerases. JFH1 (2a) S502H (A), and HCR6 (1b) H502S RdRps (C) were applied on Superdex 200 gel filtration columns in 50 mM Tris-HCl (pH 7.5), 150 mM NaCl, 3.5 mM MnCl₂, 1 mM DTT, and 0.2% glycerol. JFH1 (2a) RdRpS502H was also applied with 0.1% Triton X-100 (B). Inset in A: The fractions of the void volume—158 kDa (1), those of lower-molecular weight fractions (2), fractions C12, and D12 of JFH1 (2a) RdRpS502H gel filtrations were precipitated with TCA and analyzed by western blot. Inset in B: Fraction C3–C8 of JFH1 (2a) RdRpS502H in Triton X-100 were precipitated with TCA and analyzed by western blot. Inset in C: Fractions C4 and D12 of HCR6 (1b) RdRpH502S were precipitated with TCA and analyzed by western blot. The position of HCV RdRp is indicated by an arrowhead. The position of the pre-stained size marker is indicated on the left side of the blots.

is important for the intermolecular interaction of HCV 1b RdRp (Qin et al., 2002). HCV RdRps without the C-terminal hydrophobic domain were soluble in high-salt buffer (>300 mM NaCl; Fig. S1) (Ferrari et al., 1999). The shift to the delayed elution of gel-filtration of HCR6 (1b) RdRpwt and JFH1 (2a) RdRp S502H with Triton X-100, and HCR6 (1b) RdRpH502S may come from the interaction of the RdRps with Superdex200 gel matrix induced by the mutations and Triton X-100.

Our data of HCV RdRp oligomerization at 502H (Fig. 6) are in agreement with those by Qin et al. (Qin et al., 2002), but are contradictory to those obtained by more sensitive methods (fluorescence resonance energy transfer [FRET] and yeast two-hybrid system) (Wang et al., 2002; Clemente-Casares et al., 2011). Interactions between a charged amino acid (His) and an aromatic residue (Trp) (Fernandez-Recio et al., 1997; Matthews et al., 1997; Takeuchi et al., 2003), or His–Glu interactions (Marti and Bosshard, 2003), are often found in proteins. JFH1 (2a) RdRpwt did not form dimers (Chinnaswamy et al., 2010). 502H may interact with 125 W in α F

(Clemente-Casares et al., 2011), but not with 18E (Qin et al., 2002). This interaction is dissociated both with high-salt (Fig. S1) and with Triton X-100 (Figs. 5 and 6). Taken together, 502H of HCV 1b RdRp is important for oligomer formation in transcription (physiological salt) conditions. Besides the oligomerization using 502H, the α F and α T helices of HCV RdRp, which were proposed to be involved in oligomerization (Clemente-Casares et al., 2011), may also be involved in oligomerization of the molecules in transcription condition. The 502 mutations in HCR6 (1b) and JFH1 (2a) RdRps are likely to affect the structure of the template channel by affecting the helix structures of the thumb domain (Bressanelli et al., 2002; Chinnaswamy et al., 2008) because the polymerase and RNA template binding activity of these mutant RdRps was not activated by Triton X-100 (Figs. 3 and 4). These findings indicate the importance around amino acid 502H for HCV 1b RdRp structure. However, these data contradict to the previous reports (Qin et al., 2002; Clemente-Casares et al., 2011).

Comparing the polymerase and template RNA-binding activity of JFH1 (2a) and HCR6 (1b) RdRps with and without Triton X-100,

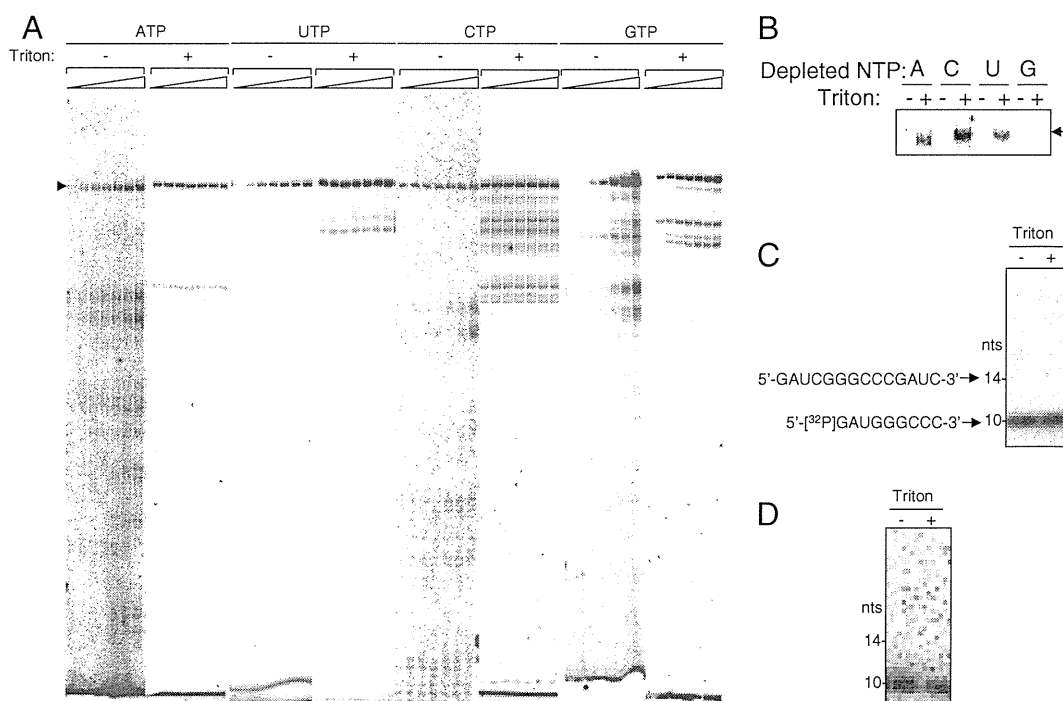


Fig. 7. Effect of substrate concentrations on in vitro transcription of HCR6 (1b) wild-type RNA polymerase, and TNTase activity in the presence of Triton X-100. **A:** Effect of nucleotide concentration on HCV HCR6 (1b) RdRpwt in vitro transcription with (+) and without (–) 0.02% Triton X-100. The concentration of ATP, UTP, and CTP varied from 1 to 50 μ M, and that of GTP varied from 5 to 500 μ M. **B:** Effect of nucleotide depletion on HCV HCR6 (1b) RdRpwt in vitro transcription with (+) and without (–) 0.02% Triton X-100. The position of 184-nt products is indicated by an arrowhead (A and B). **C:** TNTase activity of HCV HCR6 (1b) RdRpwt. 5'-[³²P]sym/sub was transcribed by HCV HCR6 (1b) RdRpwt with (+) and without (–) 0.02% Triton X-100. **D:** TNTase activity of HCV HCR6 (1b) RdRpwt. sym/sub was transcribed with [³²P]UTP by HCV HCR6 (1b) RdRpwt with (+) and without (–) 0.02% Triton X-100. The position of 10-nt sym/sub and 14-nt is indicated on the left.

RdRp which formed oligomer using 502H did not show high polymerase activity (Figs. 3–6). The inactive oligomer may be a part of the reason why a small fraction, less than 1%, of the purified HCV BK RdRp which belonged to 1b participated productively in transcription in vitro (Carroll et al., 2000). Taking together the data obtained by FRET (Clemente-Casares et al., 2011) and yeast two-hybrid systems (Wang et al., 2002), dynamic intermolecular interactions may occur under transcription conditions through the α T helix where amino acid 502 is located. The reason why only 1b RdRp was activated with Triton X-100 although RNA binding of all the RdRps tested was enhanced with Triton X-100, is not clear.

In case of JFH1 (2a) RdRp, the interaction with Triton X-100 may be different from that of HCR6 (1b) RdRp because it was not activated with Triton X-100 (Figs. 1 and 3), and because its gel-filtration profile was not affected with Triton X-100 (Fig. 5). This may be the reason of the inhibition of polymerase activity of JFH1 (2a) RdRpS502H by Triton X-100 although it was also disrupted to monomer (Figs. 3 and 6).

Triton X-100 activated only HCV 1b RdRp (Figs. 3 and 4). The closed conformation of HCV RdRp is required for de novo initiation (Chinnaswamy et al., 2008). With and without Triton X-100, JFH1 (2a) RdRpwt showed as high polymerase activity as HCR6 (1b) RdRpwt did with Triton X-100 (Fig. 3B). The very closed conformation of JFH1 (2a) RdRp is proposed to facilitate de novo initiation and high polymerase activity (Simister et al., 2009). Triton X-100 may also help the conformational change of HCR6 (1b) RdRp to the very closed conformation like that of JFH1 (2a) RdRp during transcription initiation.

HCV RdRp was co-purified with nucleic acids (Figs. S1 and S2). The contaminating nucleic acids were removed from HCV RdRp by high salt treatment. The contaminating nucleic acids carry proteins that have affinity to them, which misleads HCV in vitro transcription data. They also oligomerize HCV RdRp by crosslinking them. In a similar way, the contaminating nucleic acids in HCV RdRp preparations may mislead the binding data of HCV RdRp with other proteins.

From the activation kinetics of the detergents (Fig. 1, Table 1), the polymerase activation of 1b RdRp is likely to depend on the micelle formation of the detergent and on the direct interaction between RdRp and the detergents. The reason why the non-ionic detergent nOG did not activate the HCV RdRp is not known (Figs. 1 and 2).

The interaction mechanism of Triton X-100 and HCV 1b RdRp may be similar as that of sphingomyelin and HCV 1b RdRp because their activation kinetics were similar and the activated genotype was the same (Weng et al., 2010). Sphingomyelin activated only HCV 1b, but did not activate 1a or 2a RdRps. Both the activation curve of sphingomyelin and that of Triton X-100 showed the linear increase of polymerase activity. Then, sphingomyelin reached plateau at 20 molecules, and Triton X-100 reached plateau around its CMC.

Data about TNTase activity of HCV RdRp are controversial (Behrens et al., 1996; Ranjith-Kumar et al., 2001, 2004; Vo et al., 2004). In our system, TNTase activity was not detected with or without Triton X-100 (Figs. 7C and D).

GTP binds to HCV RdRp both as substrate and as a component of RdRp (Bressanelli et al., 2002). The apparent K_m for GTP with Triton X-100 indicated that the substrate affinity dropped as low as to lose fidelity (Table 1, Figs. 7A and B). Triton X-100 may have affected the substrate-binding although its mechanism is not clear. HCV 1b full-length RdRp transcription activity obtained with CHAPS (Wang et al., 2002) might be that without fidelity as shown with Triton X-100. Detergents should not be used while screening substrate inhibitors of HCV RdRp. These data indicate that caution should be exercised while using detergents in anti-HCV RdRp drug screening tests.

Supplementary materials related to this article can be found online at doi:10.1016/j.gene.2012.01.044.

Acknowledgments

We thank Dr. J. Bukh, Dr. C. Rice, and Dr. R. Bartenschlager for providing pJ6CF, pHCVrep13(S2204I)Neo, and Con1, respectively. This

work was supported by a Grant-in-Aid from the Chinese Academy of Sciences (O514P51131 and KSCX1-YW-10), the Chinese 973 Project (2009CB522504), and the Chinese National Science and Technology Major Project (2008ZX10002-014).

References

- Aizaki, H., Lee, K.J., Sung, V.M., Ishiko, H., Lai, M.M., 2004. Characterization of the hepatitis C virus RNA replication complex associated with lipid rafts. *Virology* 324, 450–461.
- Arnold, J.J., Cameron, C.E., 2000. Poliovirus RNA-dependent RNA polymerase (3D(pol)). Assembly of stable, elongation-competent complexes by using a symmetrical primer-template substrate (sym/sub). *J. Biol. Chem.* 275, 5329–5336.
- Behrens, S.E., Tomei, L., De Francesco, R., 1996. Identification and properties of the RNA-dependent RNA polymerase of hepatitis C virus. *EMBO J.* 15, 12–22.
- Binder, M., Quinkert, D., Bochkarova, O., Klein, R., Kezmic, N., Bartenschlager, R., Lohmann, V., 2007. Identification of determinants involved in initiation of hepatitis C virus RNA synthesis by using intergenotypic replicase chimeras. *J. Virol.* 81, 5270–5283.
- Blight, K.J., McKeating, J.A., Marcotrigiano, J., Rice, C.M., 2003. Efficient replication of hepatitis C virus genotype 1a RNAs in cell culture. *J. Virol.* 77, 3181–3190.
- Bressanelli, S., Tomei, L., Rey, F.A., De Francesco, R., 2002. Structural analysis of the hepatitis C virus RNA polymerase in complex with ribonucleotides. *J. Virol.* 76, 3482–3492.
- Carroll, S.S., Sardana, V., Yang, Z., Jacobs, A.R., Mizenko, C., Hall, D., Hill, L., Zugay-Murphy, J., Kuo, L.C., 2000. Only a small fraction of purified hepatitis C RNA-dependent RNA polymerase is catalytically competent: implications for viral replication and in vitro assays. *Biochemistry* 39, 8243–8249.
- Chinnaswamy, S., Murali, A., Li, P., Fujisaki, K., Kao, C.C., 2010. Regulation of de novo-initiated RNA synthesis in hepatitis C virus RNA-dependent RNA polymerase by intermolecular interactions. *J. Virol.* 84, 5923–5935.
- Chinnaswamy, S., Yarbrough, I., Palaninathan, S., Kumar, C.T., Vijayaraghavan, V., Demeler, B., Lemon, S.M., Sacchettini, J.C., Kao, C.C., 2008. A locking mechanism regulates RNA synthesis and host protein interaction by the hepatitis C virus polymerase. *J. Biol. Chem.* 283, 20535–20546.
- Clemente-Casares, P., Lopez-Jimenez, A.J., Bellon-Echeverria, I., Encinar, J.A., Martinez-Alfaro, E., Perez-Flores, R., Mas, A., 2011. De novo polymerase activity and oligomerization of hepatitis C virus RNA-dependent RNA-polymerases from genotypes 1 to 5. *PLoS One* 6, e18515.
- Cramer, J., Jaeger, J., Restle, T., 2006. Biochemical and pre-steady-state kinetic characterization of the hepatitis C virus RNA polymerase (NS5B Δ 21, HC-J4). *Biochemistry* 45, 3610–3619.
- Fernandez-Recio, J., Vazquez, A., Civera, C., Sevilla, P., Sancho, J., 1997. The tryptophan/histidine interaction in alpha-helices. *J. Mol. Biol.* 267, 184–197.
- Ferrari, E., Wright-Minogue, J., Fang, J.W., Baroudy, B.M., Lau, J.Y., Hong, Z., 1999. Characterization of soluble hepatitis C virus RNA-dependent RNA polymerase expressed in *Escherichia coli*. *J. Virol.* 73, 1649–1654.
- Grakoui, A., McCourt, D.W., Wychowski, C., Feinstone, S.M., Rice, C.M., 1993. Characterization of the hepatitis C virus-encoded serine proteinase: determination of proteinase-dependent polyprotein cleavage sites. *J. Virol.* 67, 2832–2843.
- Hijikata, M., Mizushima, H., Tanji, Y., Komoda, Y., Hirowatari, Y., Akagi, T., Kato, N., Kimura, K., Shimotohno, K., 1993. Proteolytic processing and membrane association of putative nonstructural proteins of hepatitis C virus. *Proc. Natl. Acad. Sci. U. S. A.* 90, 10773–10777.
- Hirschman, S.Z., Gerber, M., Garfinkel, E., 1978. Differential activation of hepatitis B DNA polymerase by detergent and salt. *J. Med. Virol.* 2, 61–76.
- Hong, Z., Cameron, C.E., Walker, M.P., Castro, C., Yao, N., Lau, J.Y., Zhong, W., 2001. A novel mechanism to ensure terminal initiation by hepatitis C virus NS5B polymerase. *Virology* 285, 6–11.
- Kashiwagi, T., Hara, K., Kohara, M., Iwahashi, J., Hamada, N., Honda-Yoshino, H., Toyoda, T., 2002a. Promoter/origin structure of the complementary strand of hepatitis C virus genome. *J. Biol. Chem.* 277, 28700–28705.
- Kashiwagi, T., Hara, K., Kohara, M., Kohara, K., Iwahashi, J., Hamada, N., Yoshino, H., Toyoda, T., 2002b. Kinetic analysis of C-terminally truncated RNA-dependent RNA polymerase of hepatitis C virus. *Biochem. Biophys. Res. Commun.* 290, 1188–1194.
- Kiyosawa, K., Sodeyama, T., Tanaka, E., Gibo, Y., Yoshizawa, K., Nakano, Y., Furuta, S., Akahane, Y., Nishioka, K., Purcell, R.H., et al., 1990. Interrelationship of blood transfusion, non-A, non-B hepatitis and hepatocellular carcinoma: analysis by detection of antibody to hepatitis C virus. *Hepatology* 12, 671–675.
- Lemon, S., Walker, C., Alter, M., Yi, M., 2007. Hepatitis C virus. In: Knipe, D., Howley, P. (Eds.), *Fields Virology*. Lippincott-Raven Publishers, Philadelphia, PA, pp. 1253–1304.
- Lohmann, V., Korner, F., Herian, U., Bartenschlager, R., 1997. Biochemical properties of hepatitis C virus NS5B RNA-dependent RNA polymerase and identification of amino acid sequence motifs essential for enzymatic activity. *J. Virol.* 71, 8416–8428.
- Luo, G., Hamatake, R.K., Mathis, D.M., Racela, J., Rigat, K.L., Lemm, J., Colonno, R.J., De, 2000. novo initiation of RNA synthesis by the RNA-dependent RNA polymerase (NS5B) of hepatitis C virus. *J. Virol.* 74, 851–863.
- Marti, D.N., Bosshard, H.R., 2003. Electrostatic interactions in leucine zippers: thermodynamic analysis of the contributions of Glu and His residues and the effect of mutating salt bridges. *J. Mol. Biol.* 330, 621–637.
- Matthews, J.M., Ward, L.D., Hammacher, A., Norton, R.S., Simpson, R.J., 1997. Roles of histidine 31 and tryptophan 34 in the structure, self-association, and folding of murine interleukin-6. *Biochemistry* 36, 6187–6196.
- Murayama, A., Date, T., Morikawa, K., Akazawa, D., Miyamoto, M., Kaga, M., Ishii, K., Suzuki, T., Kato, T., Mizokami, M., Wakita, T., 2007. The NS3 helicase and NS5B-to-3'X regions are important for efficient hepatitis C virus strain JFH-1 replication in Huh7 cells. *J. Virol.* 81, 8030–8040.
- Murayama, A., Weng, L., Date, T., Akazawa, D., Tian, X., Suzuki, T., Kato, T., Tanaka, Y., Mizokami, M., Wakita, T., Toyoda, T., 2010. RNA polymerase activity and specific RNA structure are required for efficient HCV replication in cultured cells. *PLoS Pathog.* 6, e1000885.
- Qin, W., Luo, H., Nomura, T., Hayashi, N., Yamashita, T., Murakami, S., 2002. Oligomeric interaction of hepatitis C virus NS5B is critical for catalytic activity of RNA-dependent RNA polymerase. *J. Biol. Chem.* 277, 2132–2137.
- Ranjith-Kumar, C.T., Gajewski, J., Gutshall, L., Maley, D., Sarisky, R.T., Kao, C.C., 2001. Terminal nucleotidyl transferase activity of recombinant Flaviviridae RNA-dependent RNA polymerases: implication for viral RNA synthesis. *J. Virol.* 75, 8615–8623.
- Ranjith-Kumar, C.T., Sarisky, R.T., Gutshall, L., Thomson, M., Kao, C.C. De, 2004. novo initiation pocket mutations have multiple effects on hepatitis C virus RNA-dependent RNA polymerase activities. *J. Virol.* 78, 12207–12217.
- Saito, I., Miyamura, T., Ohbayashi, A., Harada, H., Katayama, T., Kikuchi, S., Watanabe, Y., Koi, S., Onji, M., Ohta, Y., et al., 1990. Hepatitis C virus infection is associated with the development of hepatocellular carcinoma. *Proc. Natl. Acad. Sci. U. S. A.* 87, 6547–6549.
- Sakamoto, H., Okamoto, K., Aoki, M., Kato, H., Katsume, A., Ohta, A., Tsukuda, T., Shimma, N., Aoki, Y., Arisawa, M., Kohara, M., Sudoh, M., 2005. Host sphingolipid biosynthesis as a target for hepatitis C virus therapy. *Nat. Chem. Biol.* 1, 333–337.
- Schmitt, M., Scrima, N., Radujkovic, D., Caillet-Saguy, C., Simister, P.C., Friebe, P., Wicht, O., Klein, R., Bartenschlager, R., Lohmann, V., Bressanelli, S., 2011. A comprehensive structure–function comparison of hepatitis C virus strain JFH1 and J6 polymerases reveals a key residue stimulating replication in cell culture across genotypes. *J. Virol.* 85, 2565–2581.
- Shi, S.T., Lee, K.J., Aizaki, H., Hwang, S.B., Lai, M.M., 2003. Hepatitis C virus RNA replication occurs on a detergent-resistant membrane that cofractionates with caveolin-2. *J. Virol.* 77, 4160–4168.
- Simister, P., Schmitt, M., Geitmann, M., Wicht, O., Danielson, U.H., Klein, R., Bressanelli, S., Lohmann, V., 2009. Structural and functional analysis of hepatitis C virus strain JFH1 polymerase. *J. Virol.* 83, 11926–11939.
- Takeuchi, H., Okada, A., Miura, A., 2003. Roles of the histidine and tryptophan side chains in the M2 proton channel from influenza A virus. *FEBS Lett.* 552, 35–38.
- Tanaka, T., Kato, N., Cho, M.J., Sugiyama, K., Shimotohno, K., 1996. Structure of the 3' terminus of the hepatitis C virus genome. *J. Virol.* 70, 3307–3312.
- Thompson, F.M., Libertini, L.J., Joss, U.R., Calvin, M., 1972. Detergent effects on a reverse transcriptase activity and on inhibition by rifamycin derivatives. *Science* 178, 505–507.
- Tsukiyama-Kohara, K., Iizuka, N., Kohara, M., Nomoto, A., 1992. Internal ribosome entry site within hepatitis C virus RNA. *J. Virol.* 66, 1476–1483.
- Vo, N.V., Tuler, J.R., Lai, M.M., 2004. Enzymatic characterization of the full-length and C-terminally truncated hepatitis C virus RNA polymerases: function of the last 21 amino acids of the C terminus in template binding and RNA synthesis. *Biochemistry* 43, 10579–10591.
- Wang, Q.M., Hockman, M.A., Staschke, K., Johnson, R.B., Case, K.A., Lu, J., Parsons, S., Zhang, F., Rathnachalam, R., Kirkegaard, K., Colacino, J.M., 2002. Oligomerization and cooperative RNA synthesis activity of hepatitis C virus RNA-dependent RNA polymerase. *J. Virol.* 76, 3865–3872.
- Wasley, A., Alter, M.J., 2000. Epidemiology of hepatitis C: geographic differences and temporal trends. *Semin. Liver Dis.* 20, 1–16.
- Watashi, K., Ishii, N., Hijikata, M., Inoue, D., Murata, T., Miyazaki, Y., Shimotohno, K., 2005. Cyclophilin B is a functional regulator of hepatitis C virus RNA polymerase. *Mol. Cell* 19, 111–122.
- Weng, L., Du, J., Zhou, J., Ding, J., Wakita, T., Kohara, M., Toyoda, T., 2009. Modification of hepatitis C virus 1b RNA polymerase to make a highly active JFH1-type polymerase by mutation of the thumb domain. *Arch. Virol.* 154, 765–773.
- Weng, L., Hirata, Y., Arai, M., Kohara, M., Wakita, T., Watashi, K., Shimotohno, K., He, Y., Zhong, J., Toyoda, T., 2010. Sphingomyelin activates hepatitis C virus RNA polymerase in a genotype specific manner. *J. Virol.* 84, 11761–11770.
- Weyant, R.S., Edmonds, P., Swaminathan, B., 1990. Effect of ionic and nonionic detergents on the Taq polymerase. *Biotechniques* 9, 308–309.
- Wu, A.M., Cetta, A., 1975. On the stimulation of viral DNA polymerase activity by non-ionic detergent. *Biochemistry* 14, 789–795.

Geographical, genetic and functional diversity of antiretroviral host factor TRIMCyp in cynomolgus macaque (*Macaca fascicularis*)

Akatsuki Saito,^{1†} Ken Kono,^{2†} Masako Nomaguchi,³ Yasuhiro Yasutomi,⁴ Akio Adachi,³ Tatsuo Shioda,² Hirofumi Akari^{1,4} and Emi E. Nakayama²

Correspondence

Hirofumi Akari
akari@pri.kyoto-u.ac.jp
Emi E. Nakayama
emien@biken.osaka-u.ac.jp

¹Primate Research Institute, Kyoto University, Inuyama 484-8506, Japan

²Department of Viral Infections, Research Institute for Microbial Diseases, Osaka University, Suita 565-0871, Japan

³Department of Microbiology, Institute of Health Biosciences, The University of Tokushima Graduate School, Tokushima 770-8503, Japan

⁴Tsukuba Primate Research Center, National Institute of Biomedical Innovation, Tsukuba 305-0843, Japan

The antiretroviral factor tripartite motif protein 5 (*TRIM5*) gene-derived isoform (TRIMCyp) has been found in at least three species of Old World monkey: rhesus (*Macaca mulatta*), pig-tailed (*Macaca nemestrina*) and cynomolgus (*Macaca fascicularis*) macaques. Although the frequency of TRIMCyp has been well studied in rhesus and pig-tailed macaques, the frequency and prevalence of TRIMCyp in cynomolgus macaques remain to be definitively elucidated. Here, the geographical and genetic diversity of TRIM5 α /TRIMCyp in cynomolgus macaques was studied in comparison with their anti-lentiviral activity. It was found that the frequency of TRIMCyp in a population in the Philippines was significantly higher than those in Indonesian and Malaysian populations. Major and minor haplotypes of cynomolgus macaque TRIMCyp with single nucleotide polymorphisms in the cyclophilin A domain were also found. The functional significance of the polymorphism in TRIMCyp was examined, and it was demonstrated that the major haplotype of TRIMCyp suppressed human immunodeficiency virus type 1 (HIV-1) but not HIV-2, whilst the minor haplotype of TRIMCyp suppressed HIV-2 but not HIV-1. The major haplotype of TRIMCyp did not restrict a monkey-tropic HIV-1 clone, NL-DT5R, which contains a capsid with the simian immunodeficiency virus-derived loop between α -helices 4 and 5 and the entire *vif* gene. These results indicate that polymorphisms of TRIMCyp affect its anti-lentiviral activity. Overall, the results of this study will help our understanding of the genetic background of cynomolgus macaque TRIMCyp, as well as the host factors composing species barriers of primate lentiviruses.

Received 2 October 2011

Accepted 22 November 2011

INTRODUCTION

Human immunodeficiency virus type 1 (HIV-1) barely replicates in Old World monkeys such as cynomolgus macaques (CMs; *Macaca fascicularis*) and rhesus macaques (RMs; *Macaca mulatta*). This species barrier has long hampered the use of Old World monkeys for human immunodeficiency virus type 1 (HIV-1) research. Recently, a number of intrinsic anti-HIV-1 cellular factors, including

tripartite motif protein 5 α (TRIM5 α), cyclophilin A (CypA), the apolipoprotein B mRNA-editing enzyme catalytic polypeptide-like 3 (APOBEC3) family and tetherin were identified in Old World monkey cells (Nomaguchi *et al.*, 2008; Sauter *et al.*, 2010). Of these factors, TRIM5 α was found to strongly suppress HIV-1 replication, mainly by affecting the virus disassembly step, resulting in a decrease in reverse-transcription products (Nakayama & Shioda, 2010; Stremlau *et al.*, 2004). TRIM5 α contains a RING domain, a B-box domain, a coiled-coil domain and a PRYSPRY (B30.2) domain. Importantly, the PRYSPRY domain recognizes the capsid of incoming retroviruses, leading to post-entry restriction of infection. RM and CM TRIM5 α restrict HIV-1 but not simian immunodeficiency virus isolated from an infected rhesus macaque (SIVmac) (Nakayama *et al.*, 2005; Stremlau *et al.*, 2004; Yap *et al.*, 2004). In the case of HIV-2

†These authors contributed equally to this work.

The GenBank/EMBL/DDBJ accession numbers for the sequences of CM TRIMCyp-major (DK) and RM TRIMCyp are AB671588 and AB671589, respectively.

Two supplementary tables are available with the online version of this paper.

infection, viruses carrying proline (P) at aa 120 of the capsid protein are sensitive to CM TRIM5 α , whereas those with either alanine or glutamine (Q) are resistant (Song *et al.*, 2007). Both CM TRIM5 α -sensitive and -resistant HIV-2 strains are restricted by RM TRIM5 α , and three amino acid residues – threonine (T), phenylalanine (F) and P at aa 339, 340 and 341, respectively – of RM TRIM5 α are important for restricting particular HIV-2 strains, which are still resistant to CM TRIM5 α (Kono *et al.*, 2008). It is also known that TRIM5 α exhibits a high degree of sequence variation, even within macaque species. In some individual RMs, the TFP residues at aa 339–341 of TRIM5 α are replaced with a single Q (Newman *et al.*, 2006) and this TFP→Q polymorphism affects the anti-lentiviral activity of RM TRIM5 α (Kirmaier *et al.*, 2010).

Although pig-tailed macaques (PMs; *Macaca nemestrina*) have long been thought to exhibit a higher susceptibility to HIV-1 infection than RMs and CMs (Agy *et al.*, 1992), the underlying mechanism determining this difference remained unclear. Recently, a TRIM5–CypA chimeric protein, referred to as TRIMCyp, was discovered in PMs, and the monkeys exclusively expressed TRIMCyp but not TRIM5 α (Brennan *et al.*, 2008; Liao *et al.*, 2007). TRIMCyp is an alternatively spliced isoform of the *TRIM5* gene in which the PRYSPRY domain of TRIM5 α is replaced with a retrotransposed *CypA* gene. The retrotransposition of the *CypA* sequence in the 3' UTR of the *TRIM5* gene correlates with a single nucleotide polymorphism (SNP) at the exon 7 splice-acceptor site, leading to skipping of exons 7 and 8 encoding the PRYSPRY domain and splicing to the *CypA* insertion. Thus, the presence or absence of the *CypA* sequence in the 3' UTR results in expression of TRIMCyp or TRIM5 α , respectively.

In vitro analyses demonstrated that cells expressing PM TRIMCyp restricted HIV-2 but not HIV-1 infection (Brennan *et al.*, 2008; Liao *et al.*, 2007), suggesting that the characteristic isoform of the *TRIM5* gene in PMs may be one of the reasons for their greater susceptibility to HIV-1 infection. Furthermore, TRIMCyp was also identified in some individual RMs and CMs (Brennan *et al.*, 2008; Newman *et al.*, 2008; Wilson *et al.*, 2008a). RM TRIMCyp, as well as that of PMs, is unable to restrict HIV-1 infection (Wilson *et al.*, 2008a). This report also showed that the frequency of TRIMCyp in Indian RMs was approximately 25%, whilst it was not found in the Chinese RM population, suggesting a geographical deviation in the frequency of TRIMCyp (Wilson *et al.*, 2008a). In the case of CMs, although the existence of TRIMCyp has been reported (Brennan *et al.*, 2008), the allele frequency, geographical distribution and relevance in antiviral activity of TRIMCyp remain to be elucidated. As the *TRIM5* gene-related factors are expected to have an impact on the replication of retroviruses, information about the genetic background of CM TRIMCyp will contribute to our understanding of host factors composing the species barrier. In the present study, we studied the geographical, genetic and functional diversity of CM TRIMCyp originating from South-West Asia (Indonesia, Malaysia and the Philippines). We showed a geographical deviation in the frequency of

TRIMCyp. Moreover, we found SNPs in CM TRIMCyp and analysed their impact on the anti-lentiviral functions, including their effect against HIV-1, HIV-2, SIVmac and monkey-tropic HIV-1 (HIV-1mt).

RESULTS

Geographical deviation in the frequency of CM TRIMCyp

Initially, we analysed the frequencies of TRIM5 α and TRIMCyp genotypes in 126 CMs originating from three different regions – Indonesia, Malaysia and the Philippines – using a PCR-based assay designed to differentiate between the presence and absence of the *CypA* insertion (Fig. 1a) (Wilson *et al.*, 2008a). Insertion of the *CypA* gene in TRIMCyp resulted in a PCR product larger than the expected size for TRIM5 α (Fig. 1b).

As shown in Table 1, 35 of the 46 Philippine individuals were homozygous for TRIMCyp, ten were heterozygous and only one was homozygous for TRIM5 α . In contrast, only three of the 33 Indonesian individuals were homozygous for TRIMCyp, 17 were heterozygous and 13 were homozygous for TRIM5 α . Interestingly, the Malaysian population was of intermediate proportions: ten TRIMCyp homozygotes, 26 heterozygotes and 11 TRIM5 α homozygotes. As shown in Fig. 2, the percentages of individuals having each *TRIM5* genotype indicated that the frequency of TRIMCyp homozygotes in Malaysian CMs was twice that in Indonesian CMs. In contrast, the frequency of TRIM5 α homozygotes in Indonesian CMs was twice that in Malaysian CMs. Taken together, the calculated allele frequencies of TRIMCyp in the Philippine, Indonesian and Malaysian CM populations were 87.0, 34.8 and 48.9%, respectively (Table 1). Statistical analyses using a χ^2 test followed by Bonferroni correction demonstrated that the frequency of TRIMCyp in the Philippine population was significantly higher than that in the Indonesian ($P < 0.0001$) and Malaysian ($P < 0.0001$) populations. In contrast, there was no significant difference between the Indonesian and Malaysian populations ($P = 0.2295$).

It should be noted that our method failed to distinguish homozygotes from hemizygotes, especially when the subjects exhibited no polymorphisms in the *TRIM5* gene. However, hemizygosity for the *TRIM5* gene is highly unlikely for the following reasons: (i) the *TRIM5* gene is on an autosomal chromosome, (ii) there is no precedent of deletion of the *TRIM5* gene in humans or primates, and (iii) all of the three CM populations in Table 1 are in Hardy–Weinberg equilibrium for *TRIM5* genotypes.

Polymorphisms in the *CypA* domain of CM TRIMCyp

Previously, it was reported that aa 357 of CM TRIMCyp, corresponding to aa 54 counting from the methionine of